

# Developing an Accelerated Aging System for Gasoline Particulate Filters and an Evaluation Test for Effects on Engine Performance

By

James E. Jorgensen  
B.S., Naval Architecture & Marine Engineering  
United States Coast Guard Academy 2010

Submitted to the Department of Mechanical Engineering in Partial Fulfillment of  
the Requirements for the Degree of

MASTER OF SCIENCE IN NAVAL ARCHITECTURE & MARINE ENGINEERING

AT THE

MASSACHUSETTS INSTITUTE OF TECHNOLOGY

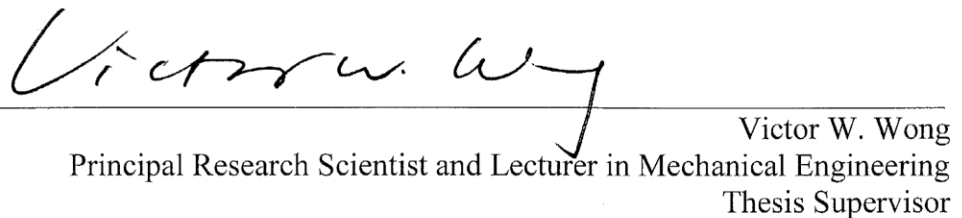
June 2014

© 2014 Massachusetts Institute of Technology  
All Rights Reserved

Signature of Author: \_\_\_\_\_

  
Department of Mechanical Engineering  
May 9, 2014

Certified by: \_\_\_\_\_

  
Victor W. Wong  
Principal Research Scientist and Lecturer in Mechanical Engineering  
Thesis Supervisor

Accepted by: \_\_\_\_\_

  
David Hardt  
Chairman, Department Committee on Graduate Students

(This Page Intentionally Left Blank)

# **Developing an Accelerated Aging System for Gasoline Particulate Filters and an Evaluation Test for Effects on Engine Performance**

By

James E. Jorgensen

Submitted to the Department of Mechanical Engineering on  
May 9, 2014 in Partial Fulfillment of the  
Requirements for the Degree of

Master of Science in Naval Architecture & Marine Engineering

## **ABSTRACT**

*Stringent regulations worldwide will limit the level of particulate matter (PM) emitted from gasoline engines equipped with direct fuel injection. Gasoline particulate filters (GPFs) present one strategy for meeting PM limits over the full operating range of the engine. Over time these filters accumulate incombustible ash, increasing system pressure drop and adversely affecting engine performance. The effect of aging as a result of ash accumulation is examined over the full lifetime of gasoline particulate filters, using a novel accelerated aging system. This system utilizes a gasoline combustion chamber into which lubricating oil is injected simulating combustion in the power cylinder – the primary source of lubricant-derived ash.*

*Advanced imaging techniques are used to characterize filter and particulate emission behavior, and compare to prior data from diesel filters of the same type. Likewise, pressure drop behavior is observed for multiple filter samples and compared to prior experiments. A collocated Gasoline Direct Injection engine was installed for comparative purposes; a method of testing engine performance with GPF installations was developed and the engine was prepared and instrumented for future testing.*

*This report details the construction and validation of the accelerated aging system, examination and comparison of results to those from prior experiments, and confirmation of principal assumptions used in developing the experimental test matrix. This study is one of a very few completed in a unique, emerging field of study, driven by new and extremely stringent emissions regulations around the globe. Practical testing here lays the foundation for future detailed research into the behavior and application of particulate filters to gasoline fueled engines in light duty passenger vehicles.*

Thesis Supervisor: Victor W. Wong

Title: Principal Research Scientist and Lecturer in Mechanical Engineering

(This Page Intentionally Left Blank)

## ACKNOWLEDGEMENTS

Completing any project of this scale is an effort which involves countless people who selflessly donate their time and knowledge to make things happen. Without each piece of this puzzle, my work at M.I.T. would not have even begun, let alone succeeded in meeting nearly every proposed goal for this project on such a short time scale.

I would first like to thank Dr. Victor Wong and Dr. Alex Sappok for their valuable support, deep knowledge of all things Particulate Filter, and ready availability to provide guidance and assistance at basically any time, day or night, during my project. Without Dr. Wong's guidance as my advisor, this project would not even exist. Without Dr. Sappok, the system would not have come together so rapidly and with so little trouble. Additionally, Dr. Justin Kamp is owed a great debt for his knowledge and expertise of the various advanced imaging methods which proved invaluable to this study.

The personnel who run the lab make things happen behind the scenes and without them, whether last minute parts orders, urgent fabrication needs, or general mechanical knowledge, this work would not have succeeded. Thane and Raymond both deserve far more credit than they ever receive.

I would also like to thank the folks with Ford Motor Company, who provided invaluable insight and technical support in the design of this experiment, as well as technical assistance in the installation and operation of our engine. Jim Pakko, Christine Lambert, Tim Chanko, Jim Warner and Christoph Borensen all provided valuable assistance to this project and deserve to be recognized for it.

My fellow students also provided much needed support and assistance, from knowing the ins and outs of the lab, to having that impossible to find part, and just providing moral support. I owe an extra debt to Tim Murray, who worked with me from start to finish to make this project happen, supplementing man hours to accomplish far more in such a short time than I could have alone.

Lastly, to the US Coast Guard for providing me the opportunity to study at M.I.T., the US Navy 2N program for giving me a home here, and my family and friends for supporting me in my studies.

(This Page Intentionally Left Blank)

# Table of Contents

ACKNOWLEDGEMENTS .....	5
List of Figures .....	11
List of Tables .....	13
List of Equations .....	13
NOMENCLATURE .....	15
1 Introduction .....	17
1.1 Spark Ignition Combustion Engines.....	17
1.1.1 Combustion Stoichiometry .....	18
1.1.2 Fuel Injection Method and Theory .....	19
1.1.3 Gasoline Engine Emissions.....	20
1.1.3.1 Nitrogen Oxides .....	20
1.1.3.2 Carbon Monoxide .....	21
1.1.3.3 Unburned Hydrocarbons .....	22
1.2 Gasoline Engine Emission Regulation.....	23
1.3 Gasoline Engine Emission Control Methods.....	25
1.3.1 Three Way Catalytic Converter .....	25
1.3.2 Particulate Filters .....	26
2 Gasoline Particulate Filters .....	27
2.1 GPF Fundamentals.....	27
2.2 Incombustible Ash.....	30
2.2.1 Lubricating Oil Consumption .....	30
2.2.2 Ash Formation.....	32
2.3 Particulate Filter Pressure Drops.....	33
2.4 Soot Fundamentals .....	35
2.4.1 Soot Formation.....	36
2.4.2 Soot Oxidation .....	37
3. Accelerated Aging System Development .....	39
3.1 Previous Gasoline Combustion Systems.....	39
3.1.1 Pulse Flame Combustor .....	39
3.1.2 Swirl Stabilized Gasoline Burner .....	40
3.2 System Design.....	41

3.2.1 Basic System Layout.....	41
3.2.2 Instrumentation .....	43
3.2.3 Particulate Filter Test Fixture.....	44
3.2.3.1 Degreening Cycle.....	45
3.2.3.2 Weight and Pressure Drop Measurements.....	45
3.3 Experimental Parameters.....	45
3.4 Experimental Design .....	47
3.4.1 Ash Finding Rate.....	47
3.4.2 Emissions Cycle Data Analysis .....	47
3.4.3 Testing Matrix .....	49
4 Accelerated Aging System Mapping.....	51
4.1 Air Tube and Nozzle Matching .....	51
4.2 Effective Range Tests .....	51
4.2.1 Low Flow Air Tube Assembly .....	52
4.2.2 High Flow Air Tube Assembly .....	53
4.2.3 Secondary Air and Heat Exchanger Effects.....	54
4.3 Accelerated Aging System Validation.....	55
4.3.1 Soot Particles.....	56
4.3.2 Ash Agglomerates.....	57
5 Engine Installation.....	59
5.1 Support Services.....	59
5.1.1 Fuel and Air Supply.....	60
5.1.2 Accessory Drive and Cooling System.....	61
5.1.3 Power Dissipation and Engine Starting .....	61
5.1.4 Engine Electrical Control .....	62
5.1.5 Instrumentation .....	62
5.2 Engine Control .....	63
5.3 Engine Performance Evaluation Test.....	63
6 Results.....	65
6.1 First Test Case – 150,000 Miles Equivalent .....	65
6.1.1 Deranged Case – Cordierite Substrate Melting .....	65
6.1.1.1 Importance of Deranged Condition Filter Test.....	67
6.1.1.2 Melted Filter Preliminary Post Mortem.....	68

6.1.2 Undamaged 150,000 Mile Equivalent Filter .....	71
6.2 Pressure Drop Summary of Intact Filters.....	72
6.3 Future Work .....	74
6.3.1 Post Mortem Analysis.....	74
6.3.2 Laboratory vs. Engine Particulate Matter Comparison.....	75
6.3.3 Powertrain Performance Analysis .....	75
7 Conclusions .....	76
7.1 Confirmation of Particulate Emission Characteristics .....	77
7.2 Validation of Equivalent Mileage Calculations .....	77
7.3 Substantiation of GPF similarity to DPF .....	77
7.4 Validation of Accelerated Aging System as Viable Test Platform .....	77
7.5 Project Continuation.....	78
REFERENCES .....	79
APPENDIX.....	82

(This Page Intentionally Left Blank)

## List of Figures

Figure 1. Actual Gasoline Particulate Filter Sample.....	27
Figure 2. Artistic Rendition of Porous Wall Filtration Process .....	28
Figure 3. Clean Cordierite Sample Showing Wall Porosity .....	28
Figure 4. Long Term Ash Build-up and Distribution - 150,000 miles equivalent GPF.....	29
Figure 5. Major Oil Consumption Mechanisms [15].....	31
Figure 6. Comparison of Actual and Predicted Filter Weight Gain vs. Oil Consumption, adapted from [16].....	32
Figure 7. Effect of Ash Load on Pressure Drop with Increasing Soot Accumulation Measured At 20,000hr <sup>-1</sup> [18].....	34
Figure 8. Deep Bed Filtration Behavior Variation Between Clean and Ash Loaded DPFs [11] .....	34
Figure 9. Combustion Chamber PM Sources in GDI Engines. Adapted from [9].....	35
Figure 10. Soot Particle Dependence on Temperature and Air-Fuel Ratio. Adapted from [9].....	37
Figure 11. Typical GPF Regeneration Process in Cake Filtration Regime, 5g/L Ash Load.....	38
Figure 12. Ignition System Arrangement.....	42
Figure 13. Accelerate Aging System Schematic Layout .....	43
Figure 14. Frequency Analysis of Combined NEDC, FTP and SFTP Test Cycle Data .....	48
Figure 15. Typical Four Hour GPF Test Loading Cycle .....	49
Figure 16. Low Flow Air Tube Assembly System Map .....	52
Figure 17. High Flow Air Tube Assembly System Map .....	53
Figure 18. Soot Threshold Exploration Test.....	54
Figure 19. Effects of Heat Exchanger and Secondary Air Introduction .....	55
Figure 20. TEM Imagery of Soot and Ash Particles from GPF Test Case .....	56
Figure 21. Magnified TEM Detail of Primary Soot Particles .....	57
Figure 22. Typical Ash Agglomerate from GPF Test Case .....	58
Figure 23. Large Ash Agglomerate from GPF Test Case .....	58
Figure 24. Ford EcoBoost 1.6L Installation.....	59
Figure 25. Melted GPF Filter Section - 150k Miles Equivalent .....	66
Figure 26. 150,000 Mile Equivalent Filter Pressure Drop Summary - Melted GPF (45,000hr <sup>-1</sup> ) .....	67
Figure 27. GPF Surface in Melted Region Showing Cracking (left) and Increased Porosity (center) .....	68
Figure 28. Individual Pore of GPF Surface in Melt Region .....	69
Figure 29. Sintered Primary Ash Particles in Melt Region.....	70

Figure 30. Large Ash Agglomerate Showing Shell-like Structure (left) and Primary Ash Particle Cut via FIB Milling to Show Complex Internal Structure (Right); Melted Filter Region .....	71
Figure 31. Individual Filter Pore with Ash Agglomerates (Left), GPF - Ash Interaction within the Pore Shown via FIB Milling (Right); Intact Filter Region.....	71
Figure 32. Pressure Drop Comparison: 150,000 Mile Equivalent Intact vs. Melted Cases (45,000hr <sup>-1</sup> )....	72
Figure 33. Pressure Drop Summary for GPF Test Samples (45,000hr <sup>-1</sup> ) .....	73
Figure 34. Pressure Drop Summary, Deep Bed Filtration Regime (45,000hr <sup>-1</sup> ).....	73
Figure A. 1 Accelerated Aging System Installation.....	83
Figure A. 2 Close Up of Accelerated Aging System Combustion Chamber .....	84
Figure A. 3 LabView Front Page Data Collection Display .....	84
Figure A. 4 15,000 Mile Equivalent Sample Pressure Drop.....	85
Figure A. 5 30,000 Mile Equivalent Sample Pressure Drop.....	86
Figure A. 6 100,000 Mile Equivalent Sample Pressure Drop.....	87
Figure A. 7 150,000 Mile Equivalent Sample Pressure Drop.....	88

## List of Tables

Table 1. United States EPA Tier 3 FTP Particulate Matter Emissions Standards. Adapted from [5] .....	23
Table 2. United States EPA Tier 3 SFTP Particulate Matter Emissions Standards. Adapted from [5] .....	23
Table 3. European Commission Euro 6 Emissions Standards. Adapted from [6] .....	24
Table 4. Degreening Cycle .....	45
Table 5. Engine Parameters .....	46
Table 6. Oil Analysis Results (Major Constituents in bold italics).....	46
Table 7. Test Filter Physical Parameters.....	47
Table 8. Major Constituent Compound Ash Transfer Rates. Adapted from [24].....	47
Table 9. Simplified GPF Loading Cycle: Underbody Configuration .....	48
Table 10. Text Matrix .....	49
Table 11. Air Tube and Nozzle Sizes .....	51
Table 12. Notional Engine Testing Program (Single Ash Load Point; MAP measured in gauge) .....	64

## List of Equations

Equation 1. Stoichiometric Combustion of Isooctane.....	18
Equation 2. Relative Air-Fuel Ratio .....	18
Equation 3. Zeldovich Mechanism [2].....	21
Equation 4. Hydrocarbon Combustion Mechanism Summary .....	21
Equation 5. Carbon Dioxide Oxidation.....	21
Equation 6. Predicted Ash Transported Per Equivalent Mileage.....	33
Equation 7. Fuel Nozzle Size Computation .....	51

(This Page Intentionally Left Blank)

## NOMENCLATURE

μm	Micrometer (meter * 10 <sup>-6</sup> )
3DCT	Three Dimensional computed tomography
AC	Alternating current
API	American Petroleum Institute
ASTM	American Society for Testing and Materials
ATI	Accurate Technologies, Incorporated
BCM	Body control module
BDC	Bottom dead center
BSFC	Brake specific fuel consumption
°C	Degrees Celsius
CI	Compression ignition
CJ-4	2007 and newer diesel lubricating oil (engine oil standard reference code)
CPSI	Channels per square inch
DI	Direct injection
DPF	Diesel particulate filter
ECM	Engine control module
EGO	Exhaust gas oxygen
EGT	Exhaust gas temperature
EPA	Environmental Protection Agency
FIB	Focused ion beam
FTP	Federal Test Procedure
Gal	U.S. Gallon (128 fluid ounces)
GDI	Gasoline direct injection
GF-5	Gasoline fueled (engine oil standard reference code)
GPF	Gasoline particulate filter
GVWR	Gross vehicle weight rating
HC	Hydrocarbon
HP	Horsepower
Hr	Hour
inHg	Inches of mercury (measurement of pressure head)
K	Degrees Kelvin
kg	Kilogram
km	Kilometer
L	Liter
LDT	Light duty truck
LDV	Light duty vehicle
MAF	Mass air flow
MAP	Manifold absolute pressure
MBT	Maximum brake torque
MDPV	Medium duty passenger vehicle
mg	Milligram
mi	Statute mile
MPa	Mega-Pascal (unit of pressure)
MPFI	Multi-port fuel injection
MY	Model year

NEDC	New European Driving Cycle
Nm	Nanometer (meter * 10 <sup>-9</sup> )
PAH	Polycyclic aromatic hydrocarbon
PCM	Powertrain control module
PCV	Positive crankcase ventilation
PI	Positive ignition (spark ignition)
PM	Particulate matter
PN	Particulate number
PPM	Parts per million
RM	Reference mass
RPM	Revolutions per minute
SAE	Society of Automotive Engineers
SCFM	Standard cubic feet per minute
SCXI	National Instruments Data Acquisition Chassis (trade name, not acronym)
SEM	Scanning electron microscopy
SFTP	Supplemental Federal Test Procedure
TCM	Transmission control module
TDC	Top dead center
TEM	Transmission electron microscopy
TMAP	Temperature / manifold absolute pressure
U.S.	United States
USB	Universal serial bus
XRD	X-ray diffraction

$\lambda$	Lambda (ratio of (A/F) to (A/F) <sub>s</sub> )
(A/F)	Air to Fuel ratio
(A/F) <sub>s</sub>	Stoichiometric Air to Fuel Ratio
C <sub>8</sub> H <sub>18</sub>	Iso-octane molecule
CH	Hydrocarbon radical of one carbon and one hydrogen atom
CO	Carbon monoxide
CO <sub>2</sub>	Carbon dioxide
H	Hydrogen
H <sub>2</sub> O	Water molecule
N <sub>2</sub>	Naturally occurring nitrogen molecule
NO	Nitrogen monoxide
NO <sub>2</sub>	Nitrogen dioxide
NO <sub>x</sub>	Gaseous mixture of nitrogen monoxide and nitrogen dioxide
O	Oxygen
O <sub>2</sub>	Naturally occurring oxygen molecule
OH	Hydroxide molecule
Pt	Platinum
RCHO	Hydrocarbon radical with attached hydrogen, carbon and oxygen
RCO	Hydrocarbon radical with attached carbon and oxygen
RH	Hydrocarbon radical with attached hydrogen
Rh	Rhodium

# 1 Introduction

Since the invention of the automobile, internal combustion engines powered by gasoline have been the powering method of choice for many manufacturers. In the United States, the majority of light duty vehicles (LDV) sold today are powered by gasoline engines. With the formation of the Environmental Protection Agency (EPA) in 1970, automobile engine emissions and fuel economy became subject to federal regulation; these standards continue to evolve and change with advances in technology.

In order to meet increasingly strict fuel economy standards within the U.S. and worldwide, automobile manufacturers continue to research new mechanical and technological methods to improve the efficiency of internal combustion engines used in LDV applications. One recent trend among these manufacturers is downsizing light duty engines, made possible using the improved power output available from turbocharging and higher compression ratios to compensate for decreased displacement. To support this trend, more precise fuel mixture control is desired, leading to the increased use of direct injection in light duty gasoline engines. These gasoline direct injection (GDI) engines are smaller and more efficient than their port fuel injected predecessors. However, they are subject to increased emissions scrutiny, as they have higher particulate matter (PM) emissions than conventional port injected engines [1].

## 1.1 Spark Ignition Combustion Engines

Gasoline powered automobile engines operate on a four stroke cycle called the Otto Cycle, named after Nicolaus A. Otto (1832-1891), who first built and ran such an engine in 1876. While significant advances in the application of this cycle have occurred over the last 130 years, the basic operating principle remains the same. At its most basic, the four stroke engine may be described as a reciprocating piston, internal combustion engine which utilizes a precisely timed electronic spark to produce in-cylinder combustion. The flow of gases in and out of the cylinder are controlled by linear-actuated poppet valves, typically configured with either two or four valves per cylinder. The cycle begins with the intake stroke, where a premixed charge of air and fuel is drawn into the cylinder by mechanical vacuum as the piston approaches the bottom dead center (BDC) position; the intake valve closes, and the piston travels to the top dead center (TDC) position. Compression ratios in typical automobile engines vary from 8:1 to 12:1, with

spark applied between 10 and 40 degrees of crank rotation angle prior to TDC to achieve maximum efficiency for given operating conditions. As the air-fuel mixture burns, the in-cylinder temperature and pressure rise, forcing the piston back to BDC in the expansion (power) stroke. In-cylinder pressures typically fall between 2 and 3 MPa (20 – 30 bar) and end gas temperatures may be as high as 3000 K (2727°C). Finally, the exhaust valve opens and the burned gas is displaced from the cylinder as the piston returns to TDC to start the intake cycle again. [2]

### 1.1.1 Combustion Stoichiometry

In ideal, stoichiometric combustion, each molecule of fuel is oxidized in the presence of precisely the correct amount of oxygen to achieve complete conversion of the fuel to combustion products. Isooctane may be used to present a close example to gasoline combustion:

#### Equation 1. Stoichiometric Combustion of Isooctane



The ratio of the mass of air to the mass of fuel consumed in each combustion event is called the Air-Fuel ratio (A/F); for a stoichiometric combustion event, the value is represented as (A/F)<sub>s</sub>. For Isooctane as shown in Equation 1, (A/F)<sub>s</sub> = 15.13; for typical gasoline (A/F)<sub>s</sub> = 14.6. [2]

Stoichiometric combustion represents the ideal, or chemically correct, combustion reaction. If either more or less air is provided per molecule of fuel, the products of the reaction change, either including un-oxidized air or un-oxidized hydrocarbon fuel. Likewise, end gas temperature and pressure are both effected by the (A/F) ratio in the combustion reaction. [2] For this reason, it is useful to define a second ratio, lambda (λ):

#### Equation 2. Relative Air-Fuel Ratio

$$\lambda = (\text{A/F})_{\text{Actual}} / (\text{A/F})_s \quad [2]$$

The ratio lambda is utilized in spark ignition engines for control of fuel supply to the engine.

### **1.1.2 Fuel Injection Method and Theory**

In spark ignition engines, engine power is regulated by throttling air intake to the cylinders and matching fuel input to the amount of air supplied. As previously described, it is ideal to maintain the ratio of fuel to air as close to stoichiometric as possible. Historically, this metering was completed using a carburetor; this device utilized a venturi-type fuel pick up to supply the correct amount of fuel to the engine. [2] In a modern engine, fuel metering is accomplished utilizing electronic fuel injection.

In the most basic implementation, electronic fuel injection utilizes simple sensory input and feedback to control the air-fuel ratio in the engine. Fuel is supplied to the engine via an external electronic pump; this fuel supply feeds the fuel rail, and is regulated to a predetermined pressure. The fuel rail supplies fuel to each individual injector. The amount of fuel delivered by the injector is determined via pulse width modulation; the engine computer (ECM) sends an electronic pulse to open the injector for a certain time period. The ECM measures air admitted into the engine using a mass airflow (MAF) sensor and pressure in the intake using a manifold absolute pressure (MAP) sensor. It receives feedback from an exhaust gas oxygen (EGO) sensor; this sensor operates on a high-low signal principle, with the signal going high when un-oxidized oxygen is detected in the exhaust. Using the information provided by the MAF and MAP sensors, the ECM utilizes programmed tables to determine the correct pulse width for the injection event. Each cycle, the pulse width is varied slightly; when the EGO signal is low it is increased, and when the EGO signal becomes high, it is decreased. This is done to maintain combustion as near stoichiometric air-fuel ratio as possible. [2]

Historically, fuel injection engines have operated using an implementation called multi-port fuel injection (MPFI), where fuel for each cylinder is injected into the intake track directly behind the intake valve; this system provides excellent fuel atomization and requires minimal injection pressure. However, fuel evaporation occurs in the intake track, so evaporative cooling effects are minimal inside the cylinder. Additionally, this method of injection results in a fuel puddle in the intake track; this causes a transient effect upon engine condition changes, whereby the air-fuel ratio becomes lean because the fuel delivery rate is dependent on the mass of the fuel puddle. [2]

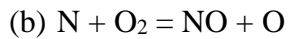
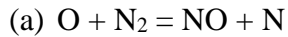
Recent trends in the automotive industry, as mentioned previously, are moving towards downsizing of engines in order to meet more stringent emissions and fuel economy standards; this is made possible through the increase of compression ratios and the use of turbochargers. This would not be feasible without the use of GDI engines. Direct injection (DI) is different from MPFI in that instead of premixing the fuel and air in the intake track, the fuel is precisely metered into the cylinder during the compression stroke. This presents several distinct advantages: first, because the fuel is injected as liquid, evaporative cooling takes place inside the cylinder, reducing compression end state temperature, allowing for higher compression ratio (and hence higher efficiency) without knocking. [2,3] Secondly, the injection of fuel directly into the cylinder allows more precise control of the air-fuel ratio, allowing a reduction in brake specific fuel consumption (BSFC), and consequently and overall improvement in fuel economy. Thirdly, because fuel is no longer entrained in the puddle mass in the intake track, transient variations in fuel delivery are essentially eliminated. [3]

### **1.1.3 Gasoline Engine Emissions**

Spark ignition gasoline engine emissions may be broadly categorized under two groups, gaseous and particulate. The majority of regulations on gasoline engine and LDV emissions have been focused on the former group in the past. The major constituents of this group are Nitrogen Oxides (NO/NO<sub>2</sub>), commonly referred to as NO<sub>x</sub>, Carbon Monoxide (CO), and unburned hydrocarbons (HC). Particulate emissions in carbureted and MFPI engines are very low and in the past, have not been regulated; rather, emissions regulations with regard to PM have focused on diesel engines. [2]

#### **1.1.3.1 Nitrogen Oxides**

The formation of NO<sub>x</sub> in spark ignition engine exhaust is dependent primarily upon exhaust stream temperature and the presence of un-oxidized oxygen particles; in spark ignition engines, the majority of the NO<sub>x</sub> emissions are composed of NO. As shown in Equation 1, for every mole of hydrocarbon fuel consumed, there is a significant quantity of N<sub>2</sub> carried into the exhaust stream (for Isooctane, over 47 moles of N<sub>2</sub> per mole of fuel); N<sub>2</sub> is naturally present in the atmosphere in these quantities. The generation of NO is governed in the combustion process by a series of equations known as the Zeldovich Mechanism [2]:

**Equation 3. Zeldovich Mechanism****[2]**

Control of these reactions is achieved largely by two methods; the first being reduction of end gas temperature and the second being minimization of excess oxygen present in the exhaust stream. The latter is accomplished by maintaining near-stoichiometric combustion; the former by adjustments to spark timing and dilution of the intake charge to reduce overall end gas temperature. [2]

**1.1.3.2 Carbon Monoxide**

Spark ignition emissions of CO are almost exclusively controlled by the air-fuel ratio of the combustion. For combustion which is fuel-lean (excess oxygen), CO levels are largely uniform; for fuel-rich combustion, CO concentration increases in an approximately linear fashion. CO is formed as part of the principal reaction steps by which hydrocarbon fuel is oxidized during combustion [2]:

**Equation 4. Hydrocarbon Combustion Mechanism Summary**

R = hydrocarbon radical

When combustion is stoichiometric, the oxidation of CO is then completed in the presence of additional O:

**Equation 5. Carbon Dioxide Oxidation**

The reaction presented in Equation 5 occurs only during the expansion stroke when temperatures are in excess of 973 K (700°C) – once the exhaust valve opens, the composition of the end state gas is essentially frozen. In fuel-rich combustion, the oxidation of CO cannot be completed

because enough O is not present in the cylinder, leading to elevated CO levels in the exhaust stream. [2]

### **1.1.3.3 Unburned Hydrocarbons**

Unburned hydrocarbon emissions from carbureted and MPFI gasoline engines operating under stoichiometric conditions can be categorized into four primary mechanisms; HC emissions also occur under fuel-rich combustion, but this is to be considered an abnormal state. The first mechanism is flame quenching, wherein the combustion within the cylinder stops when the flame front impinges on the cooler cylinder walls, leaving behind a layer of unburned fuel mixture which is cooled enough by the walls to prevent oxidation. The second mechanism is so-called crevice gasses; that is, some amount of unburned charge is forced into the gap between the piston crown, the cylinder wall, and the first piston ring. The opening to this gap is small enough to cause localized flame quenching, and the unburned mixture can then expand out of the gap during the exhaust process. The third mechanism is via absorption of fuel vapor into lubricating oil films and deposits on the cylinder walls at peak pressure, this absorbed fuel then undergoes desorption once pressure drops in the expansion stroke. The fourth and final mechanism is that of incomplete combustion due to irregularities in the cycle, either partial burn or complete misfire, or due to inadequate control of transient conditions. [2]

The presence of significant quantities of unburned HC emissions in gasoline engine exhaust can lead to the formation of soot particles; in the past, this has not been a significant problem. [2] However, with the increasingly widespread use of GDI engines, PM emissions in the form of soot are increasingly under scrutiny. Within GDI engines, there is an additional mechanism for the release of unburned HC emissions leading to soot formation – in direct injection systems, it is possible for injected fuel to impinge on pistons and cylinder walls, forming pools of fuel which do not evaporate and mix with the air completely inside the cylinder prior to combustion. This condition can lead to pool fires, which is a significantly rich combustion event and leads to soot emission; for this reason, GDI engines have elevated levels of unburned HC and PM emissions when compared to MPFI or carbureted engines. [1,3,4]

## 1.2 Gasoline Engine Emission Regulation

In the United States, the Environmental Protection Agency (EPA) is responding to the increased use of GDI engines with a new series of light duty emissions regulations, known as Tier 3 Motor Vehicle Emission and Fuel Standards. Based on data from current Federal Test Procedure (FTP) [Normal Driving] and Supplemental Federal Test Procedure (SFTP) US06 [Aggressive Driving] test cycles, the EPA has proposed a series of new limits for newly manufactured vehicles starting in Model Year (MY) 2017 [5]. In particular, these standards impose regulation on the amount of PM allowed from any newly manufactured LDV. FTP standards are summarized in [Table 1](#), and SFTP standards are summarized in [Table 2](#).

**Table 1. United States EPA Tier 3 FTP Particulate Matter Emissions Standards. Adapted from [5]**

		Units	Model Year						
			2017	2018	2019	2020	2021	2022	2023+
Phase-in		%	20*	20	40	70	100	100	100
FTP	Certification	mg/mi	3	3	3	3	3	3	3
	In-use	mg/mi	6	6	6	6	6	3	3

\*Manufacturers comply in MY 2017 with 20% of their LDV and LDT fleet under 6,000 lbs GVWR or alternatively with 10% of their total LDV, LDT, and MDPV fleet

**Table 2. United States EPA Tier 3 SFTP Particulate Matter Emissions Standards. Adapted from [5]**

		Units	Model Year							
			2017	2018	2019	2020	2021	2022	2023	2024+
Phase-in		%	20*	20	40	70	100	100	100	100
US06	Certification	mg/mi	10	10	6	6	6	6	6	6
	In-use	mg/mi	10	10	10	10	10	10	10	6

\*Manufacturers comply in MY 2017 with 20% of their LDV and LDT fleet under 6,000 lbs GVWR or alternatively with 10% of their total LDV, LDT, and MDPV fleet

The standards specified for MY2017 are based on the results from the best performing LDVs using current technology [5]. The Tier 3 standards will be phased in over a period of 7 years, with rising percentages of the U.S. LDV fleet required to meet the standards each year. [Table 1](#) and [Table 2](#) show the phase-in schedule for FTP and SFTP standards, respectively. After the phase-in process is complete, FTP standards specify a PM mass limit of 3mg/mi driven; SFTP standards are rated to 6mg/mi. One of the greatest challenges in meeting these new standards is

the requirement that a new MY vehicle must satisfy the stated In-Use standards for the entirety of its “Useful Life”, this period being specified by the EPA as either 150,000 miles and 15 years, or 120,000 miles and 10 years, as applicable [5].

In Europe, the current implementation standard is Euro 6, which is the first European emissions regulation to impose limitations on particulate emissions from gasoline engines – specifically GDI engines. Euro 6 enacts a similar regulation to the EPA Tier 3 standards, specifying a PM mass limit of 4.5mg/km (7.24mg/mi), but also goes one step further by setting a PM emission numerical count limit –  $6.0 \times 10^{11}$  particles / km ( $9.66 \times 10^{11}$  particles / mi). [6] These limits are summarized in Table 3. Some literature has been published with regards to research linking number of emitted particles to PM mass emitted for diesel particulate filter (DPF) equipped vehicles; this study found an approximate correlation of  $2.0 \times 10^{12}$  particles per mg of soot. [7] Using these values the Euro 6 numerical limit equates to 0.3mg/km (0.48mg/mi), a standard which is a full order of magnitude stricter than the PM mass limit imposed either by the Tier 3 or Euro 6 standards.

**Table 3. European Commission Euro 6 Emissions Standards. Adapted from [6]**

		Reference Mass (RM) (kg)	Limit Values			
			Mass of particulate matter (PM) <sup>(1)</sup>		Number of particles (PN)	
			L <sub>5</sub> (mg/km)		L <sub>6</sub> (#/km)	
Category	Class		PI <sup>(2)</sup>	CI	PI <sup>(2)</sup> <sup>(3)</sup>	CI
M	---	All	4,5	4,5	$6.0 \times 10^{11}$	$6.0 \times 10^{11}$
N1	I	$RM \leq 1305$	4,5	4,5	$6.0 \times 10^{11}$	$6.0 \times 10^{11}$
	II	$1305 < RM \leq 1760$	4,5	4,5	$6.0 \times 10^{11}$	$6.0 \times 10^{11}$
	III	$1760 < RM$	4,5	4,5	$6.0 \times 10^{11}$	$6.0 \times 10^{11}$
N2	---	All	4,5	4,5	$6.0 \times 10^{11}$	$6.0 \times 10^{11}$

Key: PI = Positive Ignition, CI = Compression Ignition  
<sup>(1)</sup> A limit of 5,0 mg/km for the mass of particulate emissions applies to vehicles type approved to the emissions limits of this table with the previous particulate mass measurement protocol, before 1.9.2011  
<sup>(2)</sup> Positive ignition particulate mass and number limits shall apply only to vehicles with direct injection engines.  
<sup>(3)</sup> Until three years after the dates specified in Article 10(4) and (5) for new type approvals and new vehicles respectively, a particle number emission limit of  $6,0 \times 10^{12}$  #/km shall apply to Euro 6 PI direct injection vehicles upon the choice of the manufacturer. Until those dates at the latest a type approval test method ensuring the effective limitation of the number of particles emitted by the vehicles under real driving conditions shall be implemented.'

## **1.3 Gasoline Engine Emission Control Methods**

Since the beginning of automotive emissions regulation, the primary pollutants of concern have been those of gaseous nature discussed in Section 1.1.3. The primary means of controlling these pollutants, beyond those integral to engine fuel management previously discussed, has been the use of exhaust stream catalysts, which are commonly called catalytic converters. Most typically, modern engines are fitted with three way catalysts; so called because they can reduce concentrations of CO, NO<sub>x</sub> and unburned HC simultaneously. For diesel engines, where the production of PM and soot are of primary concern, the use of particulate filters is the primary means of exhaust after treatment. [2]

### **1.3.1 Three Way Catalytic Converter**

The typical construction of a three way catalyst uses a ceramic monolith structure, containing between 30 and 60 channels per square centimeter, which is contained within a metal canister and mounted in the exhaust stream close to the engine outlet. The reactions which occur within the catalyst rely heavily on exhaust stream temperature to be enabled; thus, the function of the catalyst is impaired during cold start and warm up. Once steady state is achieved, a modern three way catalyst can achieve conversion efficiencies in excess of 90% for all three gaseous pollutants. [2]

The catalytic action of the three way catalyst is promoted via inclusion of certain noble metals within the monolith construction; achieved by trapping small metal particles in an alumina wash coat, which is normally on the order of 20µm thick. This method provides the maximum possible surface area within the monolith to increase the mass flow rate of exhaust which can be effectively converted. The primary active elements in a modern catalyst are platinum (Pt) and rhodium (Rh), with a Pt/Rh ratio which may vary between 2:1 and 17:1. Platinum is primarily active in conversion of CO and unburned HC, which occurs in stoichiometric or fuel lean exhaust; rhodium is effective in the conversion of NO<sub>x</sub> when exhaust composition is stoichiometric or fuel rich. Additionally, catalysts contain an additional compound for oxygen storage, typically NiO or CeO<sub>2</sub>. This oxygen storage behavior facilitates conversion of CO and unburned HC during fuel rich conditions, by releasing stored O<sub>2</sub> to be utilized in the conversion,

and in fuel lean conditions by absorbing excess  $O_2$ , which would otherwise reduce the rate of  $NO_x$  conversion. [2]

### **1.3.2 Particulate Filters**

Diesel engines have been equipped with particulate filters in some cases for a number of years, with widespread use in the United States beginning in 2007. [2,8] These filters are constructed using a ceramic monolith filter material, with passages which are blocked either at the front face or the rear face of the filter brick. They are often made from cordierite, and typically have approximate 200 channels per square inch. [8] This forces the exhaust stream to pass through the porous ceramic media, trapping particulate matter in the exhaust stream in the process. These filters are disadvantageous in that they cause an increase in the pressure drop of the exhaust system; however, they are effective in trapping particulate matter from diesel engines. One problem with such filtration is that the filters rapidly become plugged with combustible PM, or soot, which is produced in diesel engines at a significant rate. Soot may be burned off inside the DPF by elevating the temperature above the light off temperature, which is between 773 K and 873 K (500°C to 600°C). This oxidation process requires fuel lean combustion such that oxygen is present in the exhaust stream; additionally, it requires that the ceramic filter matrix be able to withstand combustion temperatures, which must be carefully controlled to prevent catastrophic damage to the DPF brick itself. [2]

While particulate filter technology has proven effective for diesel engines, it is an as yet untried solution to the PM emissions concerns which surround GDI engines. Historically, PM emissions from gasoline engines have been neither a concern nor subject to regulation, consequently this area has not been previously studied. Technical challenges exist for their application, as well; gasoline engine end gas temperatures may approach 3000 K (2727°C), a value significantly higher than that of diesel engines, typically 800-1000K (527°C - 727°C). Accordingly, the exhaust gas temperature are much higher in gasoline engines than in diesel. [2] These higher temperatures present a concern for the integrity of the ceramic filter matrix. Additionally, with peak combustion pressure in gasoline engines ranging from 2 – 3 MPa (20-30 bar) versus typical diesel values of 4 – 5 MPa (40-50 bar), [2] sensitivity to increases in back pressure is greater in gasoline engines.

## 2 Gasoline Particulate Filters

The application of particulate filters to diesel engines has been widespread in the United States since 2007 [8], and the reduction of PM emissions achieved has been effective in meeting stringent emissions standards worldwide. [9] Application to gasoline engines has not previously been necessary and has thus not been studied in detail [2], however, in principle the same type of filtration should be adequate to the task at hand. However, because gasoline PM emissions are of smaller size than diesel PM, a finer filter is required, creating additional pressure drop and negatively impacting performance of the overall powertrain. [1]

### 2.1 GPF Fundamentals

Since the introduction of catalytic converters and particulate filters, design optimization has come to favor the monolithic ceramic substrate bricks manufactured from a ceramic substance called cordierite ( $Mg_2Al_4Si_5O_{18}$ ). This substrate is favored for its low cost, ideal thermal shock resistance and minimal thermal expansion, as well as high melting temperature and inert nature in the harsh chemical environment present in combustion exhaust. [10] Filters of this type offer the ability to capture high percentages of PM emissions while causing minimal increase in system backpressure. Figure 1 shows a photograph of an actual GPF of the type used for testing.



**Figure 1. Actual Gasoline Particulate Filter Sample**

Monolithic ceramic filters operate by forcing PM laden engine exhaust to diffuse through the walls of the individual channels within the filter brick. This behavior is accomplished by plugging some channels at the front face (inlet) side of the filter, and the remainder at the rear face (outlet) side of the filter, creating an equal number of inlet and outlet channels. PM laden exhaust flows into the inlet channels, and gaseous exhaust passes through the porous channel walls, while PM particles cannot pass and are captured within the inlet channel. Captured PM is largely transported to the rear of the filter, creating what is usually called a plug. Figure 2 shows an artistic rendition of this wall filtration process, while Figure 3 shows an image, taken via Transmission Electron Microscopy (TEM), of the clean cordierite substrate. This sample displays a wall thickness of approximately 100 $\mu\text{m}$ , with typical pore sizes in the 10-20 $\mu\text{m}$  range.

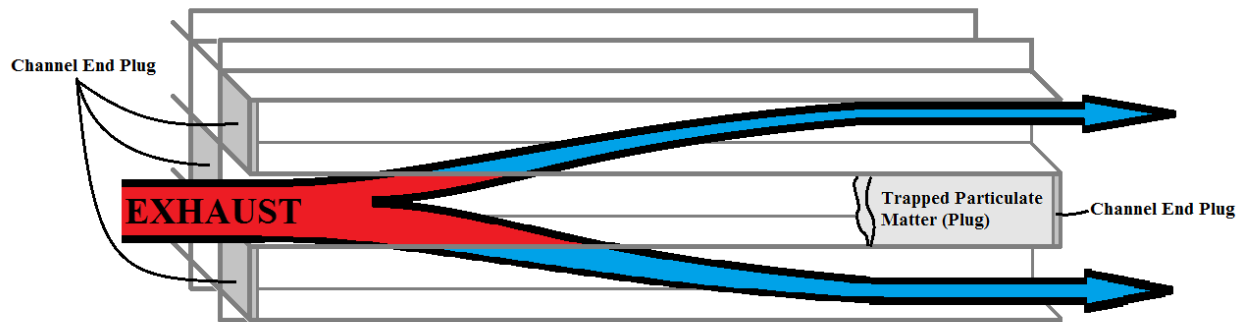


**Figure 2. Artistic Rendition of Porous Wall Filtration Process**

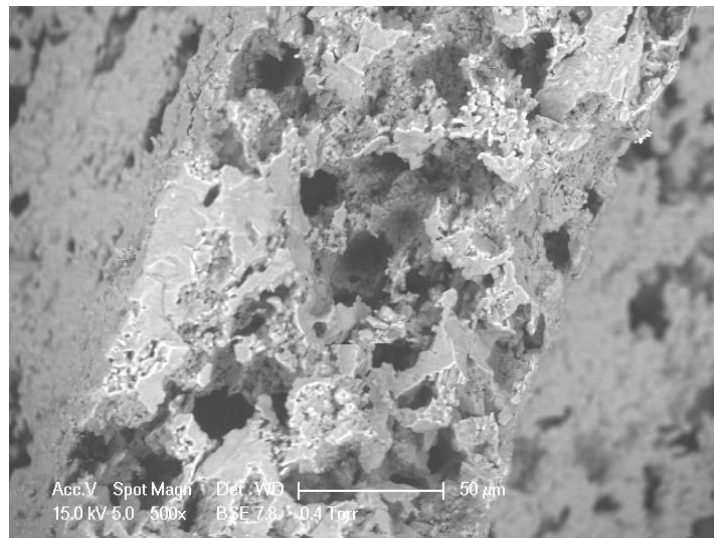


**Figure 3. Clean Cordierite Sample Showing Wall Porosity**

When the filter substrate is new, the initial phase of filtration is referred to as deep bed filtration, where the PM being removed from the exhaust stream is actually trapped inside the pores of the channel walls. After this initial deposition period, PM begins to form a layer on the surface of the channel walls and is transported to the PM plug at the rear of the channels. Filters which have primarily captured ash exhibit lower pressure drops than those which are capturing exclusively soot during this initial phase. [11] Soot particles make up the majority of PM emissions from combustion engines, and as such accumulate much more rapidly inside the filter. However, soot is combustible and can be purged from the filter channels through sufficient elevation of temperature in the presence of O<sub>2</sub>. In practice, this process requires trap temperatures in excess of 823 K (550°C) to effectively occur (without the presence of a catalyst), which may not occur during normal vehicle operation and thus may require a regeneration cycle to occur prior to the build-up of excess soot and unacceptably high back pressure levels. [12]

Once regeneration is complete, the filter contains only incombustible ash. [Figure 4](#) shows this ash distribution inside of a GPF sample aged to 150,000 miles in a laboratory setting.

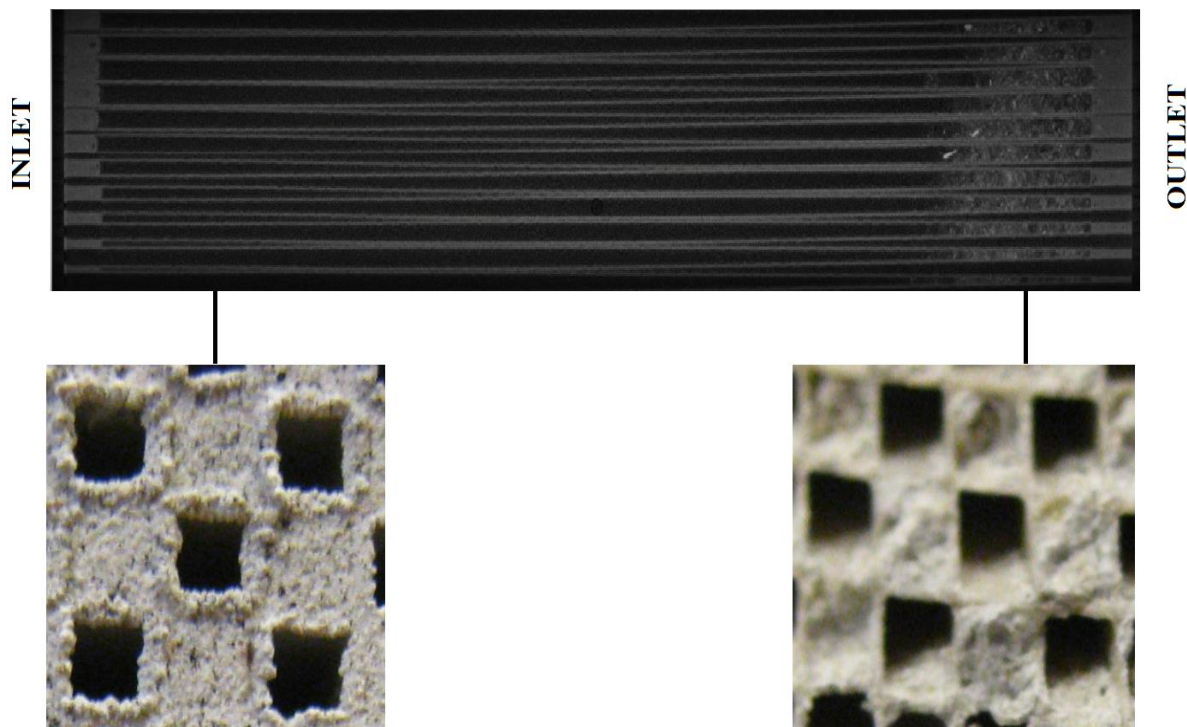


**Figure 4. Long Term Ash Build-up and Distribution - 150,000 miles equivalent GPF**

Over time, the ash deposits accumulated in the filter forming the plug begin to completely obstruct the channels close to the outlet of the GPF. The distribution image is captured using a three-dimensional computed tomography (3DCT) scan technique which allows visualization of the ash contents inside a filter brick without dissecting the filter; the images showing ash buildup on the channel walls are taken after dissection.

## **2.2 Incombustible Ash**

As soot is oxidized within the GPF, what is left behind is incombustible ash. The source of the incombustible ash within the filter has been studied extensively, and is largely traced to elemental metal compounds contained in lubricating oils. [13] In a modern, spark ignition engine, the primary methods by which lubricating oil is consumed are well defined and rates have been measured in recent studies. [14,15]

### **2.2.1 Lubricating Oil Consumption**

The consumption of oil within a spark ignition engine is well documented. To understand consumption of oil, it is informative to review the lubrication mechanisms within the engine with which they are associated. It is also important to understand the regulation of lubrication within the cylinder. In a typical spark ignition light duty engine, the lubrication of the piston and liner are regulated by a piston ring pack made up of three rings; collectively, the piston and rings are referred to as the piston assembly. The first and second rings, referenced from the crown of the piston, are compression rings and of a single piece construction. These rings are designed to have a tight fit to the liner and minimal space for bypass of compressed gas. The third, or lowest ring, is the oil control ring. This ring is typically composed of three components; an upper and lower thin metal ring, which act to carry oil to the liner during upward travel and to wipe oil from the liner during downward travel, and a central ring, called an expander, which acts to support the upper and lower components and maintain positive contact with the liner. The purpose of the oil control ring is to meter oil to the ring pack, such that sufficient lubrication exists to support the piston adequately against side loading, yet oil transport into the chamber is minimized. [2]

Three major oil consumption mechanisms may be quantified within the engine; these are blow-by, evaporation and oil transport. The importance of blow-by consumption, whereby oil is

transported in gases which leak past the piston ring pack, increases with engine load and speed, but is small compared to the other mechanisms. [14, 15] Oil evaporation is the second largest contribution to the consumption of oil within the engine; oil films which develop on the piston liner are subjected to evaporation and subsequent combustion within the chamber. This mechanism is largely controlled by temperature of the oil seal ring and piston liner and may contribute between 30 and 40 percent of total oil consumption. The largest contribution to engine oil consumption comes from oil transport, which is composed of valve guide leakage and piston ring pack leakage. [15] These major mechanisms are illustrated in [Figure 5](#).

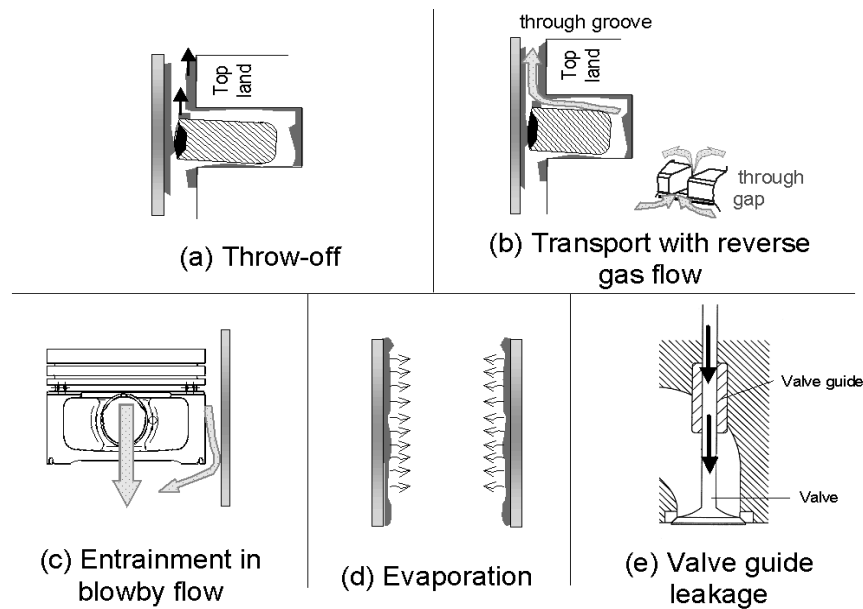


**Figure 5. Major Oil Consumption Mechanisms [15]**

As described previously, the piston ring pack is designed to control and minimize transport of oil into the cylinder; however, due to manufacturing tolerances and other variations in geometry, this control is not perfect. Liquid oil transport constitutes 40 to 50 percent of oil consumption within the cylinder, and is the dominant consumption mechanism at load conditions below 50 percent. [15]

For a modern combustion engine, of 2L displacement and four cylinders, the total contribution of the liquid oil transport may be as high as 27 grams per hour of operation. [14] As oil transport is the largest contributing factor to oil consumption, and is dominant at low load conditions most usually encountered during regular driving, it is the primary mode of oil consumption which was chosen for simulation in this study.

## 2.2.2 Ash Formation

Incombustible ash that is captured is composed of residues from multiple sources, which can include engine wear particles and residual species derived from lubricant combustion, such as sulfates, phosphates, and metallic oxides of metals such as calcium, magnesium, and zinc that are commonly present in commercial engine oils. These compounds are transported to the GPF via in-cylinder combustion of lubricant oil. [13]

One method which has been used to estimate the transfer of lubricant components to the exhaust stream is a correlation of sulfated ash content, wherein the amount of sulfated ash contained in the oil is multiplied by the amount of oil consumed to derive a value of ash mass trapped in the GPF. This method has been tested in multiple studies in the last decade; these studies have found that the sulfated ash calculation method over-estimates mass transfer to the exhaust stream. [13,16] Typical findings from studies of this type are shown in [Figure 6](#).

Several mechanisms have been proposed for this effect; the most likely explanation is that the base oil is more volatile than the metallic additives within the oil, and thus is more readily consumed in the engine. This is supported by published studies, which have found that the concentration of metallic additives in the sump oil increases with time. It is also likely that some of these metallic additives may accumulate inside the engine and exhaust track before becoming trapped in the GPF. The rate at which different additives are consumed varies depending on the component considered. [13]

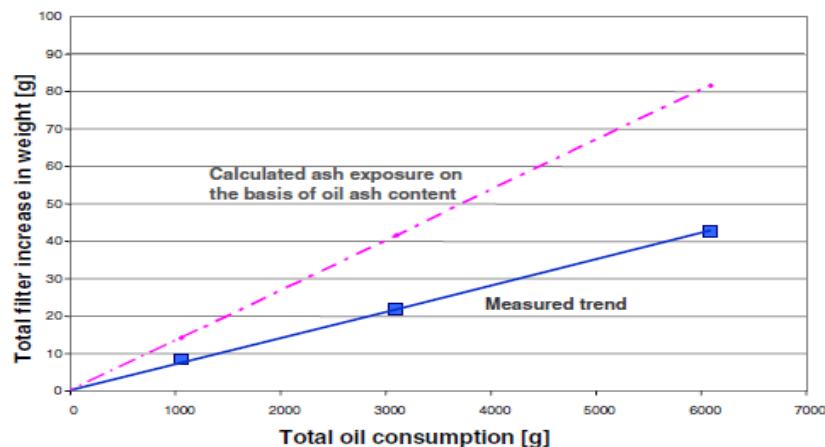


**Figure 6. Comparison of Actual and Predicted Filter Weight Gain vs. Oil Consumption, adapted from [16]**

To correct for the observed trend, the ash calculation method was modified using an *Ash Finding Rate*, which is based on ash-forming elements within the elemental composition of the oil used, and transport rates for different elements found in literature. [13,16,17] Various studies have reported ash finding rates between 35% and 67% in testing on diesel engines with DPFs. [13]

#### **Equation 6. Predicted Ash Transported Per Equivalent Mileage**

$$ASH_{\text{Equiv}} = [\text{Sulfated Ash Content}] * [\text{Oil Consumption}] * [\text{Equivalent Distance}] * [\text{Ash Finding Rate}]$$

In Equation 6, sulfated ash content is taken from analysis of the test oil via the American Society for Testing and Materials (ASTM) D874 method; oil consumption is a manufacturer provided number for the engine being evaluated; equivalent distance is given in miles of driving for the filter test point, and ash finding rate is determined using individual component transport rates based on elemental oil analysis via ASTM D5185. In this study, only major constituents of the lubricant package were considered.

### **2.3 Particulate Filter Pressure Drops**

Particulate filters are of significant interest in the development of Tier 3/Euro 6 compliant GDI engines because of their ability to capture soot from the exhaust stream. However, as discussed in Section 2.1, this ability comes with the price of increased exhaust back pressure. From work with DPFs, it is known that the back pressure of a particulate filter increases as the filter captures PM from the exhaust stream. Soot captured in the filter may be oxidized, but incombustible ash builds up in the filter and causes the pressure drop to increase over the life of the filter. [18,19]

Figure 7 shows the pressure drop behavior of DPFs with various ash loading levels as the mass of trapped soot is increased, demonstrating the detrimental effects of high ash loads.

In the early stages of filtration, particulate filters exhibit what is called deep bed filtration behavior. This regime is characterized by rapid pressure increase due to penetration of PM into the pores of the filter substrate; this behavior is typical during initial accumulation of PM. Once deep bed filtration has occurred, the trapped PM begins to form a layer, or cake, which is more porous and thus the rate of increase of pressure drop with PM loading decreases, relative to the deep bed filtration regime. It has been noted in previous studies that the deep bed filtration

regime effects are reduced in those filters which contain ash; that is, the initial rise in pressure drop is much smaller. This effect is due to the early penetration of ash into the pores of the substrate; ash particles are smaller and more readily penetrate the substrate, and this effect promotes earlier formation of a filtration cake. [11]

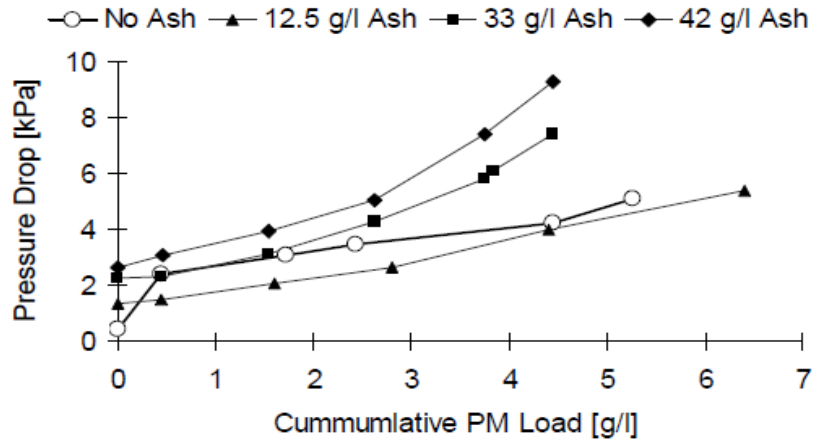


**Figure 7. Effect of Ash Load on Pressure Drop with Increasing Soot Accumulation Measured At 20,000hr<sup>-1</sup> [18]**

The result of this behavior is that filters containing some ash exhibit a lower degree of pressure drop increase as soot load rises, increasing the amount of PM which can be trapped before pressure drop levels become unacceptable; the effect can be seen in [Figure 8](#). This is particularly important for gasoline engines, which are more sensitive to back pressure than diesels. [2,11]

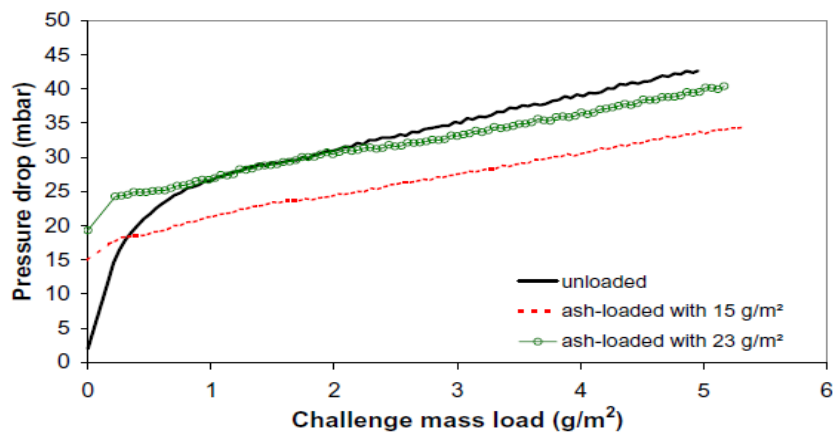


**Figure 8. Deep Bed Filtration Behavior Variation Between Clean and Ash Loaded DPFs [11]**

It is important to note that these effects are observed in PM mass relative to filter size; for common cylindrical filters such as those used in this study, the ratio is typically in grams per liter of filter volume. Such a ratio, as in [Figure 8](#), may also be reported in grams per filtration area. The beneficial effects of ash filtration are a function of filter size, and the effect diminishes as the filter becomes filled with ash, as shown in [Figure 7](#). This effect must be considered when selecting the size of a particulate filter for a particular powertrain and expected lifetime.

## 2.4 Soot Fundamentals

Soot is the major constituent of PM emissions from combustion engines, at some load conditions it may constitute greater than 99 percent of emissions entering a particulate filter. [20] Soot is a carbon-based combustible particle formed during fuel rich combustion, which typically presents in small, spherical particles forming clusters called agglomerates. Soot particles act as carriers for other particulate emissions of engines, in particular, by becoming a vector for metallic ash to be deposited in a particulate filter. [9] As mentioned in [Section 1.1.3.3](#), soot emissions in GDI engines largely originate from component wetting within the combustion chamber during the injection cycle. [4,9] [Figure 9](#) gives a visual representation of the major potential sources of particulate emissions in a typical GDI engine, including component wetting, localized rich burn of the injector charge, and also from absorption and desorption in cylinder deposits as described in [Section 1.1.3.3](#).

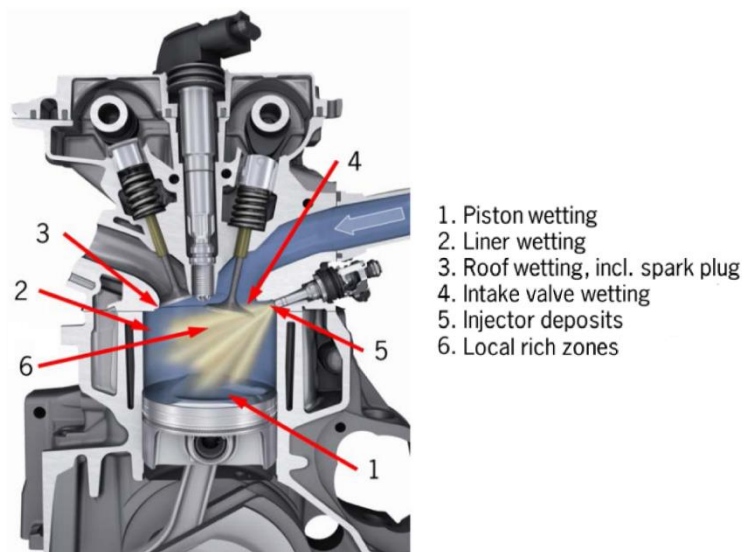


**Figure 9. Combustion Chamber PM Sources in GDI Engines. Adapted from [9]**

### 2.4.1 Soot Formation

Soot formation in engines is a fundamental process which can occur during the oxidation of hydrocarbon fuels. Specifically large hydrocarbons (e.g. isooctane,  $C_8H_{18}$ ) break down into smaller radicals during oxidation, which can include methyl ( $CH_3$ ), ethyl ( $C_2H_5$ ), and under fuel rich conditions, ethin ( $C_2H_2$ ), which is the lowest analogue of acetylene. Acetylene may also be present through a second mechanism called pyrolysis, wherein hydrocarbon molecules break down into radicals without actually oxidizing. [2,9] Acetylene is known to be one of the primary constituents of a recombination process wherein other hydrocarbon radicals ( $CH$  and  $CH_2$ ) react with  $C_2H_2$  to form polycyclic aromatic hydrocarbon (PAH) molecules, which leads to soot particle nucleation. [9]

Once soot particle nucleation has occurred, two growth mechanisms exist by which larger soot particles are formed. The first method, called surface growth, is a mechanism where existing soot nuclei attract and condense additional radicals and PAH in the chamber gas, in such a way that the soot mass grows, but the number of particles remains constant. The second method is coagulation, wherein particles collide and coalesce, such that the mass of soot remains constant but the particle number decreases. [2,9]

Gas temperature during combustion plays a critical role in the formation of soot particles; specifically, both precursor radical formation and pyrolysis rate are effected by temperature. More importantly, soot formation is highly dependent on the air-fuel ratio in the combustion chamber (which can be locally rich even during overall stoichiometric combustion). [9] This dependence is easily explained; the precursors of soot particle nucleation are hydrocarbon radicals which are readily oxidized in the presence of sufficient oxygen, thus if near stoichiometric conditions exist the precursors will be consumed before the nucleation and growth processes can be completed. [2] [Figure 10](#) gives a graphical representation of these dependences.

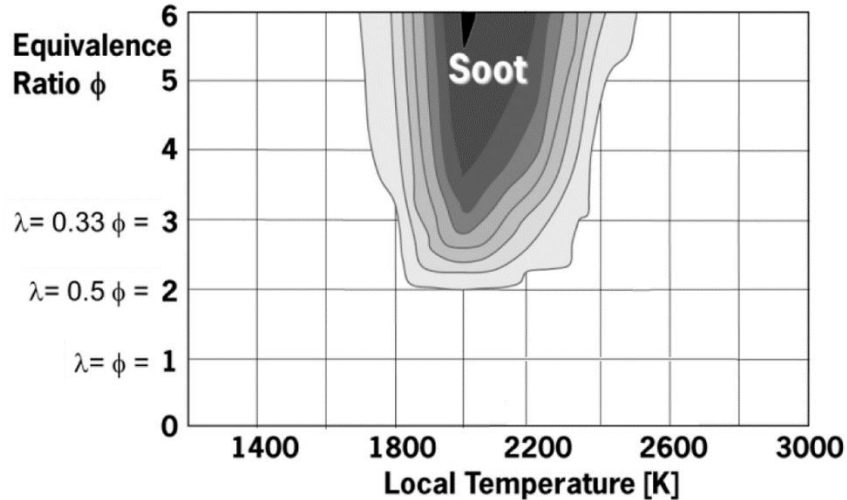
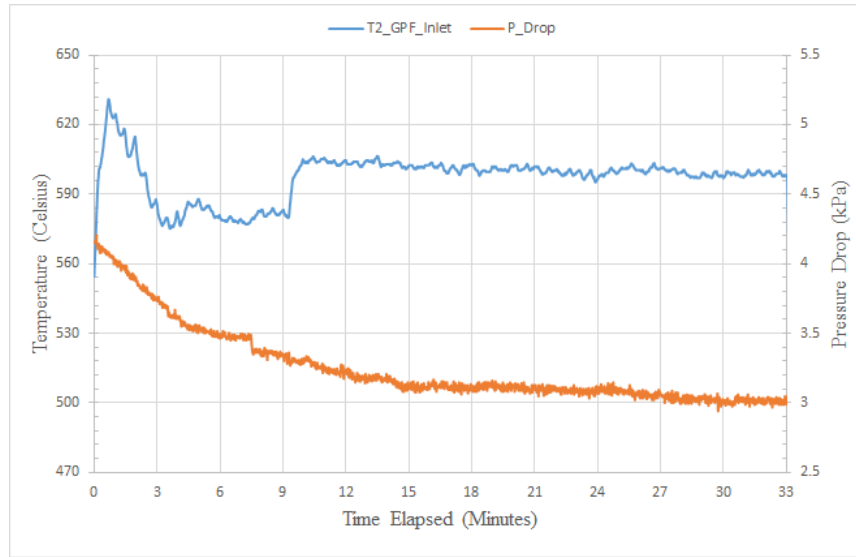


Figure 10. Soot Particle Dependence on Temperature and Air-Fuel Ratio. Adapted from [9]

## 2.4.2 Soot Oxidation

Soot particles fully formed in the combustion chamber, which are not oxidized during expansion, are transmitted to the exhaust stream and subsequently trapped in the GPF. Because soot composes the majority of particulate matter entering a filter [20], it is necessary for the soot to be oxidized in-situ in order to reduce pressure drop induced through soot accumulation, as that shown in [Figure 7](#). In order to complete this process, the GPF temperature must exceed particulate matter ignition temperature, 773 K to 873 K (500°C to 600°C), in the presence of sufficient oxygen content. [2] This process is kinetically controlled, whereby the soot particle is heated sufficiently to permit oxidation of the carbon and hydrogen contained within the structure; oxidation of the soot is irreversible once converted to CO [9], at which point the oxidation products leave the GPF under gaseous form. This process is managed by controlled elevation of the GPF temperature in the presence of lean combustion products; a typical regeneration process measured on a GPF with 5g/L of ash, falling in the cake filtration regime discussed in [Section 2.3](#), and a starting soot load of approximately 1g/L, is shown in [Figure 11](#). The oxidation of soot is a highly exothermic process, and the level of soot in the filter must be controlled not only for pressure drop, but also to prevent excess energy release during regeneration which can lead to filter cracking, ash sintering, or even melting of the cordierite substrate. In DPF applications, this soot ceiling is typically 5 – 6g/L. [8].



**Figure 11. Typical GPF Regeneration Process in Cake Filtration Regime, 5g/L Ash Load**

### **3. Accelerated Aging System Development**

The use of the diesel particulate filter (DPF) on diesel engines for PM emissions control has been studied extensively and systems have been retrofitted since the 1980's. [2] In the United States, DPFs have seen widespread use on diesel engines since 2007. These filters offer excellent trapping efficiency for both soot and inorganic ash compounds in the exhaust stream [8]. However, application to gasoline engines has not been necessary in the past, and is now a subject of interest due to the increasingly stringent emissions regulations and increased use of GDI engines, as previously described.

In order to evaluate the behavior of gasoline engines when using GPFs, it is necessary to complete tests with filters throughout the various stages of the 150,000 mile life to which they will be certified. Because the impending implementation of stringent PM standards worldwide, and due to the number of tests desired, it is not practical to field age all of these samples. Therefore, to facilitate the study of lifetime behavior of GPFs and the effects on overall powertrain performance, the development of accelerated aging system for GPFs was desirable. Such a system had previously been developed and validated to test DPFs using diesel fuel at M.I.T. [21]; with this basic design in mind, a review of existing laboratory gasoline combustion systems was conducted.

#### **3.1 Previous Gasoline Combustion Systems**

Two major types of gasoline-combustion capable laboratory systems are presently in use for catalyst and other emissions system component testing. Each system is unique and designed for a specific purpose; review of these designs led to the implementation of new modifications to M.I.T.'s previously developed accelerated aging system for diesel fuel.

##### **3.1.1 Pulse Flame Combustor**

The first common type of gasoline laboratory combustion system is called a pulsator, short for pulse flame combustor. This system was originally developed, by adaption of a different system design, for the rapid and economic evaluation of automotive catalyst designs in the 1970's. The device is designed to create a steady flow of carefully controlled exhaust gases, simulating the flow of spark ignition engine combustion exhaust. [22]

The present pulsator variation is composed of three components; a wick assembly, an ignition furnace and a reaction section. The wick is saturated with fuel and maintained at a temperature near, but below, the fuel boiling point to promote vaporization of the fuel. The wick is placed in a flow of premixed oxygen and nitrogen; additional oxygen is introduced downstream for air-fuel ratio control. The flow then enters the ignition furnace, which is maintained between 923 K and 1273 K (650°C to 1000°C), and ignites; the flame propagates back towards the wick and collapses. A new charge of fuel-air mixture flows into the furnace, pushing the combustion gasses to the reaction section. The reaction section is also held at a specified temperature, and houses a sample section of the catalyst to be evaluated. [22]

The pulsator system is effective for the intended purpose; however, the size of the system is limited, as it was designed for testing small samples, not complete catalysts. For this reason, it is not well suited for use in a system which is designed to simulate full-scale engine exhaust testing.

### **3.1.2 Swirl Stabilized Gasoline Burner**

The second type of laboratory system used is of a swirl-stabilized burner design. This system has been developed in the last decade for the purpose of testing and aging full scale automotive catalyst designs. This development is due to requirements for automotive manufactures to certify emissions compliance of vehicles for longer and longer periods. [5,23]

The swirl stabilized burner is composed of a combustion chamber, a heat exchanger, and a test section. The combustion chamber contains a plenum, which directs airflow to a swirl plate; this plate is co-located with an air assisted fuel injector. The swirl plate creates an optimized airflow pattern within the combustion tube, allowing the air – fuel mixture to pass over the source of ignition and exit the tube to flow downstream to a heat exchanger, and then oil may be injected into the flow prior to reaching a catalyst. The system is driven by an external blower forcing air through the plenum and combustion chamber [23].

The swirl stabilized burner provides for full scale exhaust generation to age a catalytic converter; as such, it was an ideal parent design for a GPF accelerated aging system. However, the system was designed to run full scale tests in real time; for this reason, only components of the design

were used as concepts for the new system. Specifically, the ignition system design from this burner was utilized.

## **3.2 System Design**

In order to properly mimic the exhaust emission characteristics of a gasoline engine, it is necessary to understand the basic mechanisms by which oil is consumed in such an engine; these mechanisms are described in [Section 2.2.1](#). Liquid oil combustion from oil transport was selected as the mode to be simulated in the accelerated aging system; previous investigation at M.I.T. has shown that injection of oil directly into combustion best mimics this consumption mechanism. [21]

### **3.2.1 Basic System Layout**

An accelerated aging system for the study of DPF behavior had previously developed at M.I.T. for diesel fuel combustion [21]; this system provided the fundamental layout of the new accelerated aging system. Using the same model of commercial fuel oil burner as in previous experiments [8,21], a new combustion chamber was constructed to facilitate the use of gasoline as a fuel. Because gasoline is a highly volatile fuel, which is readily vaporized and oxidized, the conventional self-sustaining flame used in fuel oil burners would not support continuous combustion; the flame would simply collapse when ignition was removed. Based on the swirl-stabilized burner system previously selected as a parent design, an ignition system using continuous spark provided by automotive spark plugs was selected [23].

To adapt the system for continuous spark ignition, a cylindrical extension was provided on the original combustion chamber, allowing the placement of three spark plugs equidistant around its perimeter. The air supplied by the commercial burner is passed over a swirl plate at the injection point; the spark plugs are placed downstream of the injection point by one diameter of the chamber extension. This placement allows the induced swirl of the charge inside the combustion chamber extension to pass directly over the spark plugs. The injector utilized here is of a non-air assisted type; rather, the nozzle is of a high pressure, hollow spray pattern type. The ignition and injection arrangement is shown in [Figure 12](#). Three ignition coils are used, of a continuous duty type normally used in natural gas heating appliances; these coils supply a 6kV spark at 60Hz.

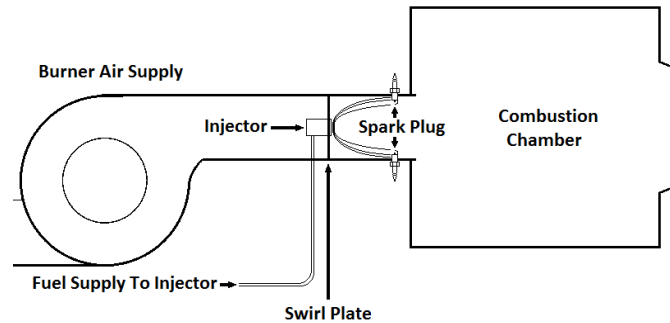


**Figure 12. Ignition System Arrangement**

Because of its high volatility, gasoline cannot be supplied by the same high pressure, positive displacement, gear-type pump as diesel; therefore, an external automotive fuel injection pump is utilized to supply fuel to the burner system via a mechanical fuel regulator and safety shut-off solenoid. The burner is provided with a 32 gallon fuel cell, allowing for operational periods in excess of 12 hours without refueling. The commercial fuel oil burner is provided with an optical safety interlock; once flame is established, if at any time during operation the light of the flame is extinguished, the control system secures the fan-driven air supply and closes the fuel shut-off solenoid. In order to maintain continuous combustion, the commercial oil burner's thermostat is replaced with a simple "on-off" switch.

The combustion chamber also houses an external, air assisted oil injector. This injector allows precisely controlled injection of engine oil into the chamber, simulating the combustion of lubricating oil in the GDI engine during regular driving cycles. This injector is composed of two components, an injector body and a nozzle. The injector body admits compressed air and oil separately; the air stream is fed around the perimeter of the nozzle, while oil is injected through the air stream. This provides for a high rate of oil atomization to enhance combustion of the lubricating oil. Oil pressure is provided by a low displacement, slow speed piston type pump for precise injection rate control. Compressed air is provided at 15PSIG, which generates a slight suction within the nozzle, such that oil pressure remains at approximately 0PSIG. This pressure is monitored during operation; if nozzle deposits begin to form, oil pressure will rise and the nozzle must be cleaned or replaced.

Downstream of the combustion chamber, the system is fitted with a tubular shell type heat exchanger, allowing regulation of the exhaust temperature during continuous operation, controlling GPF inlet temperatures for regular loading and regeneration periods. After the heat exchanger, a valve is provided to allow introduction of clean (secondary) air, to allow burner-independent regulation of exhaust stream oxygen content. A valve is then provided to allow introduction of exhaust from the co-installed Ford EcoBoost engine, just upstream of the GPF. Downstream of the GPF, an additional air inlet is provided to regulate system back pressure, and to allow exhaust cooling prior to the centrifugal blower which drives the system. The centrifugal blower is driven by a variable frequency motor control, allowing precise adjustment of blower speed; the blower is equipped with a water cooled shaft bearing to allow for high process temperatures experienced during GPF loading. A schematic layout of this system is provided in [Figure 13](#); photographs of the system are provided in the Appendix, Figures A.1 and A.2.

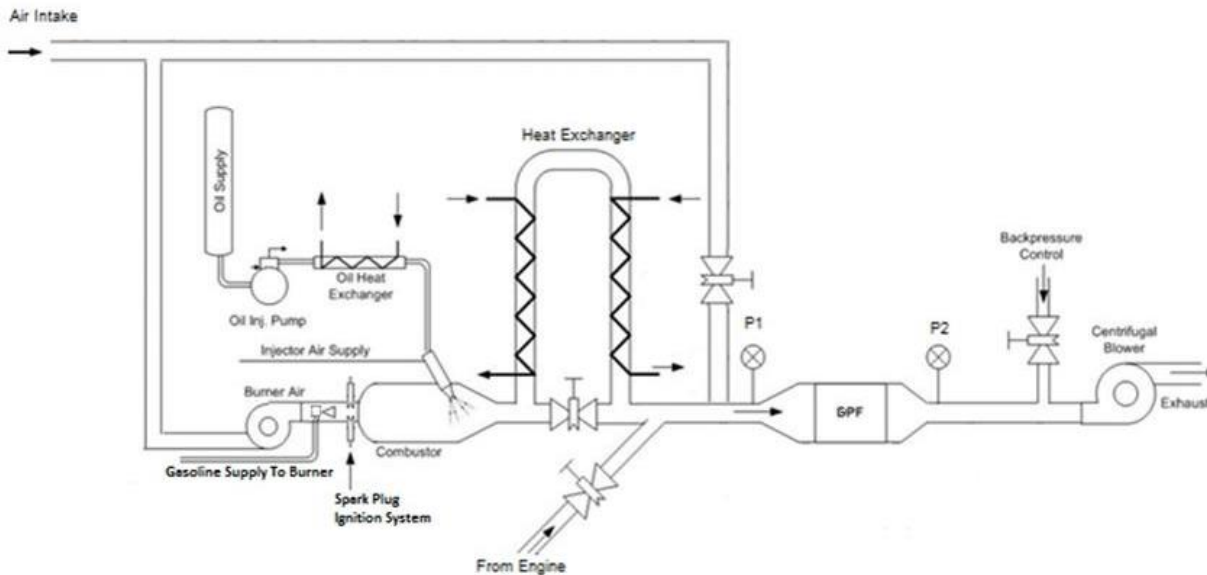


**Figure 13. Accelerate Aging System Schematic Layout**

### 3.2.2 Instrumentation

In order to accurately monitor burner behavior during ash loading, the advanced aging system is fitted with a number of data acquisition sensors. Temperature history data is recorded at various points in the system to monitor component performance. Temperature is measured at the outlet of the combustion chamber, to monitor the stability and overall health of combustion, as well as

rate of soot production. The next measurement is at the outlet of the heat exchanger, followed by the GPF inlet; this allows for regulation of exhaust stream temperature to maintain ideal GPF temperatures. Temperature is also monitored at the GPF outlet, to indicate the status of regeneration processes and ensure GPF internal temperatures are not too high. For system safety purposes, temperature of oil flow at the lubricant injection point and flow temperature into the centrifugal blower are also monitored.

Parameters relevant to system performance and aging processes are also measured. Pressure is recorded upstream and downstream of the GPF, to give real time pressure drop data. Volumetric exhaust flow is measured at the system air inlet; thus reported SCFM values are given at ambient (standard) temperature. Exhaust air-to-fuel ratio, relative to stoichiometric, ( $\lambda$ ) is measured directly upstream of the GPF, allowing for precise measurement of conditions in the GPF during normal loading and regeneration phases. Oil flow rate is measured via graduations on the oil storage cylinder, giving good indication of overall oil consumption rate.

With the exception of oil flow rate, all parameters are monitored and recorded via a National Instruments SCXI component chassis system, integrated through LabView software. A view of the LabView data acquisition program is provided in the Appendix, Figure A.3.

### **3.2.3 Particulate Filter Test Fixture**

Prior to commencing the loading of a filter specimen, the filter is mounted in a test fixture. The fixture is composed of four components; entry and exit cones which transition smoothly from exhaust to filter diameter and vice versa, and two cylindrical halves which are bolted together around the filter to securely hold it in the exhaust flow. The components are sealed with high temperature graphite sheeting gaskets to ensure leak free operation. The filter is sealed into the canister using thermal insulation matting; the matting is cut and affixed to the filter before installation in the fixture, ensuring a complete seal with no gaps where the cut ends meet. The entry and exit cones also provide mounting for inlet and outlet thermocouples previously described.

### 3.2.3.1 Degreening Cycle

Once the fixture is assembled, the thermal matting must be heated to allow for expansion and sealing of the GPF into the fixture. This is accomplished using a three step process; the filter is held in the exhaust flow at a constant flow rate and increasing temperature for a total time of three hours; this process is summarized in [Table 4](#). No oil is injected during the degreening process.

**Table 4. Degreening Cycle**

Phase	Temperature	Flow Rate	Time	Total Time
1	Cold Flow*	30 SCFM	30 minutes	30 minutes
2	400°C	30 SCFM	45 minutes	1 hour 15 minutes
3	600°C	30 SCFM	1 hour 45 minutes	3 hours

\*Cold Flow occurs with heat exchanger utilized 100%; this has a typical value of 200°C – 250°C

### 3.2.3.2 Weight and Pressure Drop Measurements

Once degreened, the filter and fixture assembly is weighed to obtain a clean reference weight. Filter weights are taken at 150°C, thus entrained moisture is not a factor in the recorded weights. For accuracy, each filter is weighed three times and the results averaged to obtain the weight; from this weight, cycle loading rate and current filter load may be calculated from the clean filter reference weight. The clean reference weight is taken immediately following degreening, before any ash loading has taken place.

For each loading cycle, pressure drop data is also recorded. The filter is allowed to cool to ambient temperature, and then pressure drop across the filter is recorded for a series of flow steps from zero to 80 SCFM, in increments between five and ten SCFM held for 60 seconds each. The clean reference pressure drop is taken following the degreening process, and each successive pressure drop is taken following a loading cycle.

## 3.3 Experimental Parameters

The accelerated aging system was developed with the intention of rapidly aging GPF test filters to evaluate performance effects and filter behavior under conditions typical to gasoline engines. Specifically, based on Tier 3 lifetime emission standard requirements shown in [Table 1](#) and [Table 2](#), aging to a maximum life of 150,000 miles and to lesser mileage equivalence for filter analysis purposes. The testing conducted was designed to evaluate options for use on a

production Ford Motor Company 1.6L EcoBoost engine; basic engine parameters are summarized in [Table 5](#).

**Table 5. Engine Parameters**

Model	1.6L EcoBoost
Maximum Torque	184 lbs-ft @ 2500 RPM
Maximum Power	178 HP @ 5700 RPM
Number of Cylinders	4, in-line
Injection System	Direct Injection
Aspiration	Turbocharged with intercooler
Displaced Volume	1.6 liters
Compression Ratio	10.1:1
Cylinder Head Layout	4 valves/cylinder, Variable Camshaft Timing (both cams)
Engine Oil Specified	SAE 5W20 Synthetic Blend, API GF-5
Engine Oil Consumption	1 quart in 10,000 miles

Because this experiment was designed to mimic production behavior of the 1.6L EcoBoost, only one oil formulation was used across all testing. The oil specified for this engine, as shown in [Table 5](#), was utilized; it is a fully formulated motor oil which is commercially available and is the factory oil fill for this engine. Detailed analysis of this oil was conducted for utilization in the experiment design; for the purposes of this testing, only major ash forming constituents were considered. The results of this testing is summarized in [Table 6](#).

**Table 6. Oil Analysis Results (Major Constituents in bold italics)**

Compound	Result	Units	Test Procedure
<i>Boron</i>	<i>186</i>	<i>PPM</i>	<i>ASTM D5185</i>
<i>Calcium</i>	<i>2289</i>	<i>PPM</i>	<i>ASTM D5185</i>
<i>Magnesium</i>	<i>8</i>	<i>PPM</i>	<i>ASTM D5185</i>
Molybdenum	14	PPM	ASTM D5185
Sodium	5	PPM	ASTM D5185
<i>Phosphorous</i>	<i>711</i>	<i>PPM</i>	<i>ASTM D5185</i>
<i>Zinc</i>	<i>817</i>	<i>PPM</i>	<i>ASTM D5185</i>
<i>Sulfated Ash</i>	<i>1.02</i>	<i>Mass Percentage</i>	<i>ASTM D874</i>

The particulate filter to be used was specified by Ford Motor Company as the primary geometry of consideration for use with the 1.6L EcoBoost engine. The filter is a standard cylindrical section geometry manufactured from cordierite, which is tailored to match engine size and

exhaust flow rates according to desired parameters. The specifications of this filter are shown in Table 7.

**Table 7. Test Filter Physical Parameters**

Length	Diameter	Channels/in <sup>2</sup> (CPSI)	Volume	Material	Catalytic Coating
5.51 in	4.66 in	220	1.5 L	Cordierite	None

### 3.4 Experimental Design

The stated goal for this system is to age a GPF to a 150,000 mile equivalent life. Based on correlation between sulfated ash content and DPF ash content weight as discussed in Section 2.2.2, Equation 6 can be utilized to determine the ash loading (in g/L) required for an individual filter to achieve the desired equivalent mileage. In order for this calculation to be completed, it is necessary to determine Ash Finding Rate.

#### 3.4.1 Ash Finding Rate

From the detailed oil analysis which was completed and is summarized in Table 6, it is possible to compute an Ash Finding Rate for this particular oil, according to transfer rates measured in previous DPF studies. [24] To do this, the measured ash transfer rates for each individual constituent compound is multiplied against its percentage composition in the oil – in essence, a weight average of the ash transfer rates. Using the values summarized in Table 8, the Ash Finding Rate for this oil is 37%.

**Table 8. Major Constituent Compound Ash Transfer Rates. Adapted from [24]**

Element	Boron	Calcium	Magnesium	Phosphorus	Zinc
Ash Transfer Rate	5%	37%	31%	46%	37%

Continuing this analysis using Equation 6, an ultimate test loading of 150,000 equivalent miles results in a filter load of 30.5 g/L for the selected GPF test geometry.

#### 3.4.2 Emissions Cycle Data Analysis

In order to facilitate repeatable loading parameters for the series of filters to be loaded, it was desirable to create a simplified loading cycle. The cycle was intended to represent the expected, averaged conditions which a GPF mounted in an underbody position might experience. The

position of the filter is particularly relevant to temperature history, as the distance the exhaust gases travel from the engine allows for additional cooling of the exhaust stream.

To select the cycle, a review was conducted of applicable emissions data from both the New European Driving Cycle (NEDC) and the FTP and SFTP test cycles mentioned previously. Temperature data from all three cycles was combined in a frequency analysis; this information is displayed in [Figure 14](#). Flow rate data for the GPF was averaged across each test, and then a weighted average was completed to select a representative flow rate.

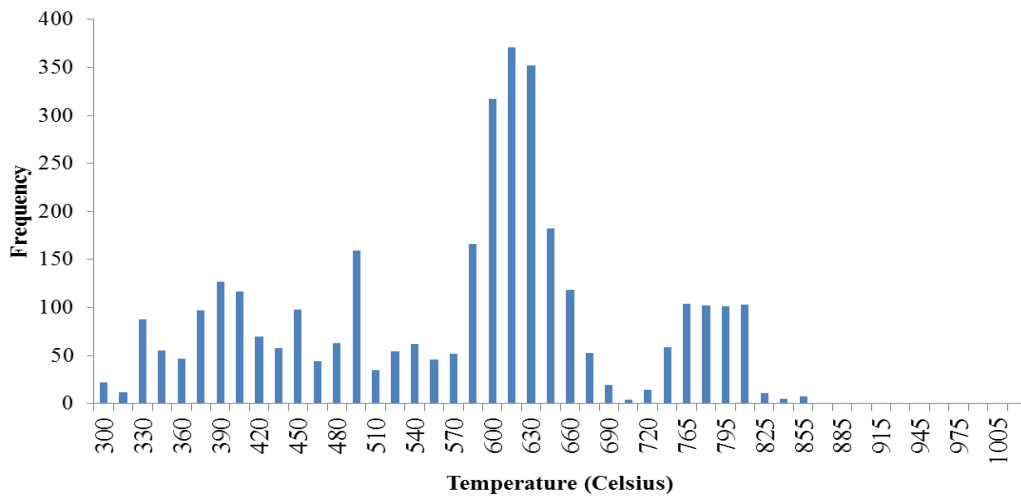


**Figure 14. Frequency Analysis of Combined NEDC, FTP and SFTP Cycle Data (Provided by Ford)**

The result of this data analysis was the selection of two representative temperature operating points, and a single operating flow rate. Temperatures represent the average driving condition, and the regenerative condition, which might be experienced on an actual vehicle. Flow rate represents the most likely conditions which would exist under regular driving. The simplified cycle parameters are summarized in [Table 9](#); [Figure 15](#) shows temperature and airflow data from a typical loading cycle.

**Table 9. Simplified GPF Loading Cycle: Underbody Configuration**

Total Cycle Time	4 hours
Normal Loading Period	3 hours, 30 minutes
Normal Loading Temperature	400 degrees Celsius
Regenerative Period	30 minutes
Regeneration Temperature	650 degrees Celsius
Cycle Flow Rate	35 SCFM
Target Ash Loading Rate	0.2 g/L-Hr

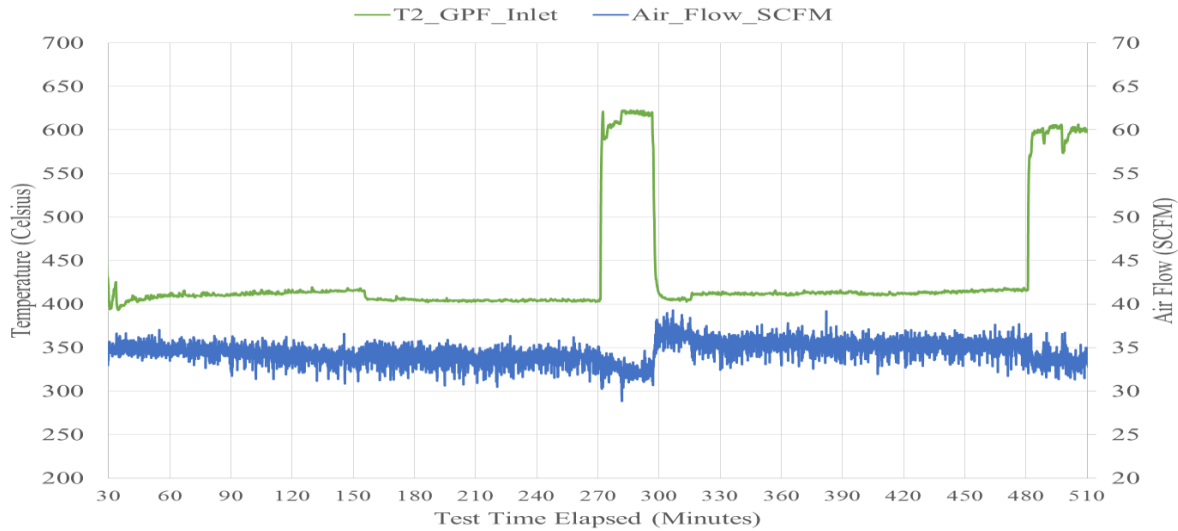


**Figure 15. Typical Four Hour GPF Test Loading Cycle**

### 3.4.3 Testing Matrix

To fully evaluate the effects of a GPF installation on powertrain performance, it is necessary to understand the behavior of the filter under typical loading conditions over the entirety of its life expectancy; in this case, the design length is 150,000 miles. For this test, it was decided to utilize a total of five separate GPFs for this evaluation purpose. Filters would be loaded according to mileage, starting with the highest mileage sample and working to the lowest. The initial design of this experiment called for the five filters to be spaced at even intervals; each successive filter would add 30,000 equivalent miles.

Once the system validation test case, a 150,000 mile sample, was loaded, the experimental test matrix was modified. Because filter behavior in the cake filtration regime was essentially linear, and behavior in the deep bed filtration regime was subject to much more rapid change in pressure drop behavior, the matrix was adjusted to provide better resolution in the deep bed filtration regime. Both the original test matrix and the adjusted, final matrix used in this study are summarized in [Table 10](#).

**Table 10. Text Matrix**

Matrix	Filter 1	Filter 2	Filter 3	Filter 4	Filter 5
Original Proposed	30,000 miles	60,000 miles	90,000 miles	120,000 miles	150,000 miles
Final Test	15,000 miles	30,000 miles	60,000 miles	100,000 miles	150,000 miles

(This Page Intentionally Left Blank)

## 4 Accelerated Aging System Mapping

In order to create a comprehensive picture of the capabilities of the accelerated aging system, a series of tests were conducted to determine the effective range at which the burner could be operated. In order to offer maximum system flexibility, all available commercial burner configurations were investigated during this process.

### 4.1 Air Tube and Nozzle Matching

The commercial burner utilizes a throttle plate inside the air inlet, both to prevent backwards flame propagation in the event of malfunction, and also to restrict the volumetric flow of air into the combustion chamber. Two different sizes of throttle plate are available. Each throttle plate size has a matched swirl plate assembly; the throttle and swirl plate assembly is fitted inside the air inlet tube. Additional adjustment of airflow into the combustion chamber is accomplished by setting the depth to which the throttle plate is seated into the air inlet tube supporting collar; all testing was conducted with a fixed depth setting. For each throttle plate, a basic calculation was conducted to determine the appropriately sized nozzle (rated in U.S. Gallons per hour):

#### Equation 7. Fuel Nozzle Size Computation

$$\text{Nozzle Size} = \frac{([\text{Air Flow Rating}] \times [\text{Inlet Air Density}])}{([\text{Air/Fuel Ratio}] \times [\text{Fuel Density}])}$$

In this calculation, air flow was converted to cubic feet per hour, a stoichiometric Air/Fuel ratio of 14.7 was utilized for gasoline, air density was measured in pounds per cubic foot, and fuel density in pounds per gallon. [Table 11](#) summarizes nozzle size selection.

**Table 11. Air Tube and Nozzle Sizes**

Air Tube Size	Rated Nozzle Size	Nozzle Type
Low Flow	0.75 U.S. gal/hr.	45° hollow pattern
High Flow	1.75 U.S. gal/hr.	45° hollow pattern

### 4.2 Effective Range Tests

Each swirl plate and nozzle combination was tested through the full range of operation, to establish system operating limits. A GPF filter was in place in the exhaust stream for the range testing, to ensure that the results obtained would best reflect actual operation of the system. Each

operating point was held for five minutes, to allow the system to reach and operate at steady state for sufficient time to achieve a base line for that operating point.

Operating points were defined using four system controls: Heat exchanger bypass percentage, secondary air percentage, vacuum relief valve position, and centrifugal blower drive frequency. These controls allow the precise regulation of test section temperature, flow rate, and oxygen content. In order that the effect of individual system controls might be evaluated, each individual test varied only one parameter.

Testing was performed by igniting the burner in a steady state condition at a set centrifugal blower frequency, and then varying the chosen system control parameter until the system either became unstable, or the flame collapsed. The burner was then re-lit, and the test proceeded to the opposite end of the range for the selected frequency, and so on for each frequency tested.

#### 4.2.1 Low Flow Air Tube Assembly

The first set of tests were conducted using the low flow air tube assembly. These tests ranged from 20Hz to 35Hz driven speed, in 5Hz increments. The resulting data was then plotted to generate a graphical system map for future testing reference; this data is displayed in [Figure 16](#).

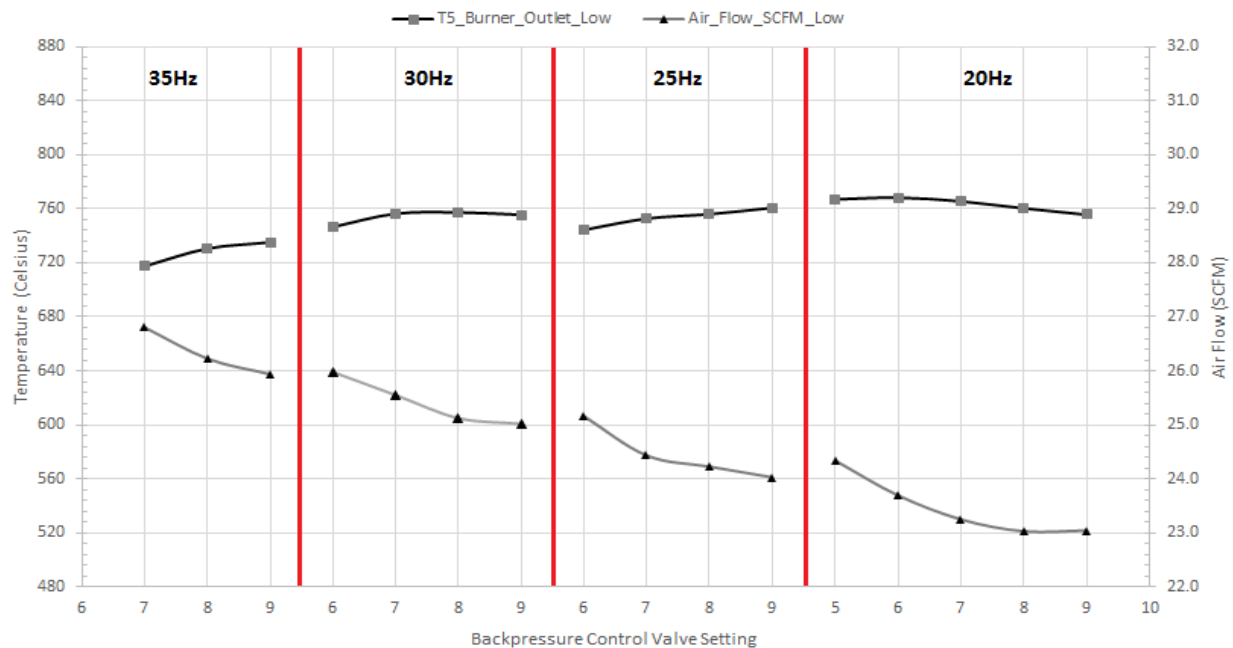


**Figure 16. Low Flow Air Tube Assembly System Map**

This air tube assembly exhibited a flow range limit of approximately 23 to 27 SCFM, with peak temperature occurring at approximately 24 SCFM; this corresponds to a slightly lean of stoichiometric air-fuel ratio.

It was noted during these tests that as the flow rate increased, the burner was more likely to become excessively lean and combustion would collapse; at lower flow rates, the temperature of the gasses entering the centrifugal blower began to exceed the rated temperature of the blower. The low flow air tube assembly, after mapping was complete, was found to admit too little air to pass through the combustion chamber for testing a GPF of the volume selected for this test.

### 4.2.2 High Flow Air Tube Assembly

As with the low flow assembly, the high flow air tube assembly was tested through a range of system settings. The assembly was tested from 30Hz to 50Hz blower speed; the system capabilities were mapped in the same way as the low flow air tube assembly, and these results are displayed in [Figure 17](#).

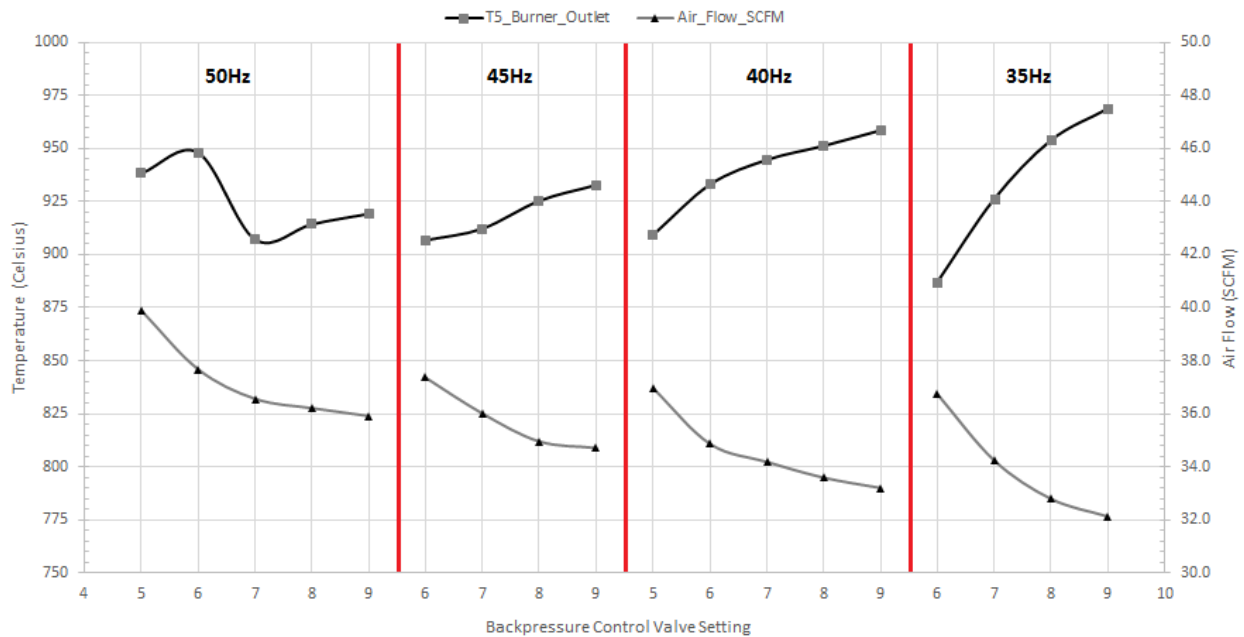


**Figure 17. High Flow Air Tube Assembly System Map**

This burner configuration exhibited a characteristic flow range between 32 and 40 SCFM in the normal system map. System operation below 32 SCFM is possible for degreening purposes. A

peak temperature setting was not observed during the system mapping process; however, under further use and observation with secondary air introduction, a peak temperature of 1373 K (1100°C) has been observed.

During the 30Hz phase of testing with the high flow air tube assembly, a phenomena best described as the *soot threshold* was quantified. Specifically, when operating the gasoline burner there exists a temperature, approximately 973 K (750°C), below which soot production from the burner becomes excessive and leads to rapid clogging of the GPF and ultimate failure of the test cycle. Burner operation at outlet temperatures as low as 773 K (500°C) are possible and were explored, however this region is not useful for the current experimental tests. This exploration is summarized in [Figure 18](#).

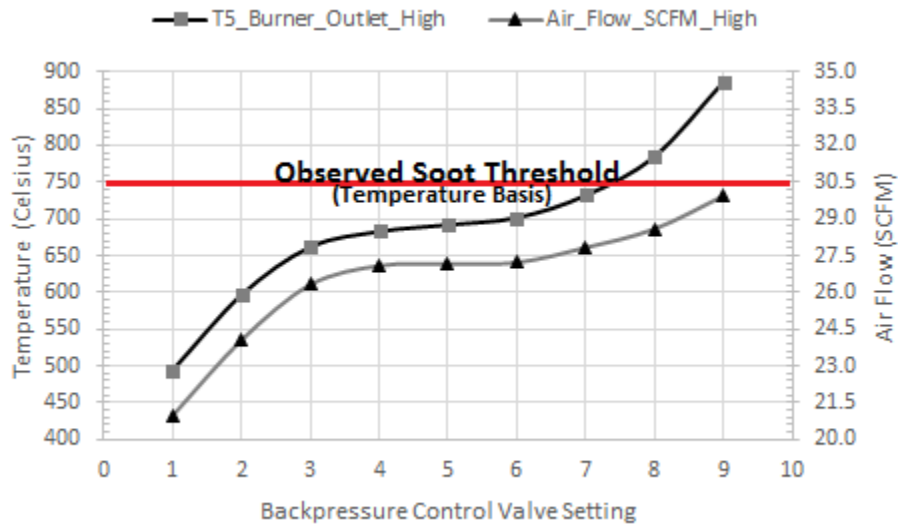


**Figure 18. Soot Threshold Exploration Test**

### 4.2.3 Secondary Air and Heat Exchanger Effects

Once the ranges of the two flow assemblies were established, a fixed point was selected using the low flow air tube assembly to determine the effects of secondary air introduction and heat exchanger application on the test section temperature. [Figure 19](#) shows the effect of secondary air introduction; as expected, the temperature of the test section drops in inverse proportion to the air flow as secondary air is introduced. It was also noted that the effect of secondary air is much more pronounced at lower percentages of introduction. Secondary air is included in the total air flow measurement reported.

Figure 19 also shows the effect of the application of the heat exchanger. Air flow rises steadily as the heat exchanger utilization is increased; as expected due to decrease of temperature passing through the centrifugal blower. Heat exchanger utilization is not reported beyond 67% because expected test section temperature history does not require full utilization of the heat exchanger; additionally, due to the physical proximity of the heat exchanger regulation valve to the combustion chamber, some difficulty was experienced with backpressure pulsation and flame collapse at utilizations approaching 100%.

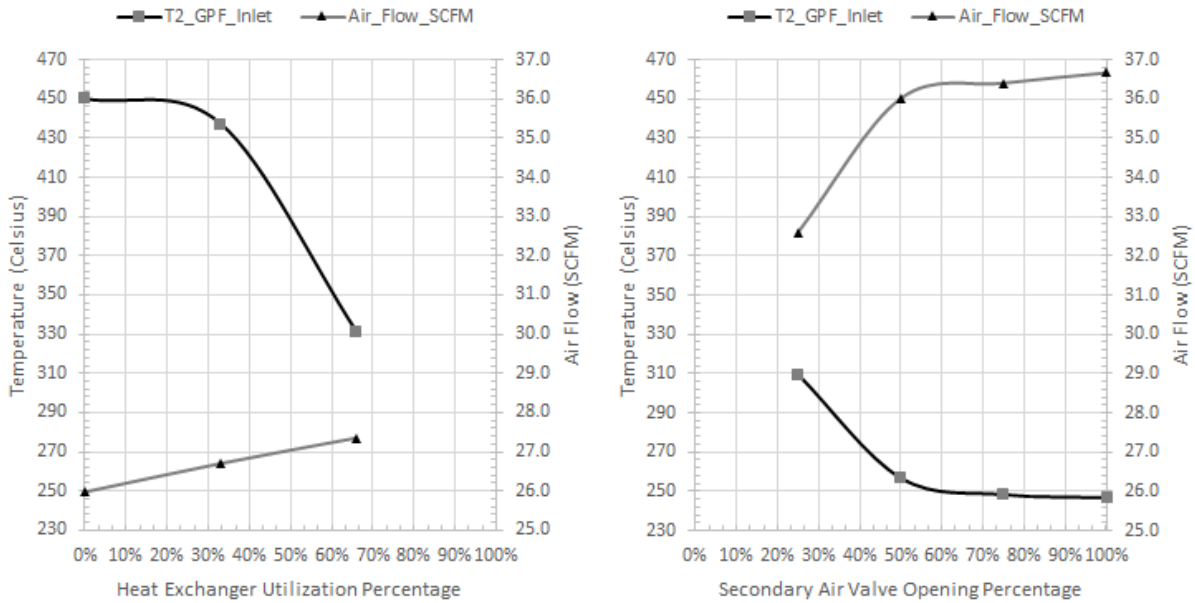


Figure 19. Effects of Heat Exchanger and Secondary Air Introduction

Similar tests were conducted with the high flow air tube assembly; with the high flow assembly in place, it is possible to operate the accelerated aging system with heat exchanger utilization at 100%; this configuration yields an achievable test section temperature range from 498 K to 973K (225°C to 700°C).

### 4.3 Accelerated Aging System Validation

Once system mapping was complete and test parameters had been selected, a series of tests were conducted using a sacrificial GPF in the test section, to collect samples of soot and ash for analysis and comparison to prior results for system validation. Samples were collected from the

sacrificial GPF after an 8 hour loading cycle, both before and after regeneration; each sample was collected from near the inlet of the GPF channels.

### 4.3.1 Soot Particles

Using TEM techniques, detailed imaging was conducted to show the general shape and size scale of the ash and soot particles found in this test case. When taking TEM images of PM, ash particles and agglomerates appear as large, dark, dense particles of varied shape, while soot appears as smaller, lightly colored spheres. [Figure 20](#) shows a TEM image of two ash agglomerates, with accompanying soot particles, taken from samples collected prior to regeneration to show soot particles.

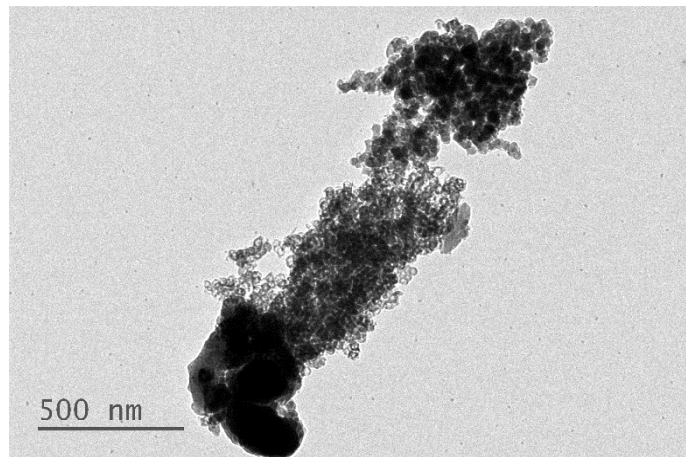


**Figure 20. TEM Imagery of Soot and Ash Particles from GPF Test Case**

In order to more accurately examine soot particles, additional TEM imagery was taken at higher magnification. Specifically, previous analysis of primary soot particles in road aged samples (as well as DPF laboratory samples) has shown a typical particle diameter between 18nm and 28nm [21]; examination of particles collected from the test case GPF show a typical particle diameter of approximately 20nm. [Figure 21](#) gives good visual confirmation of these measurements; with primary soot particles well correlated to those previously found the accelerated aging system proved to generate soot particles similar to those from an actual engine.

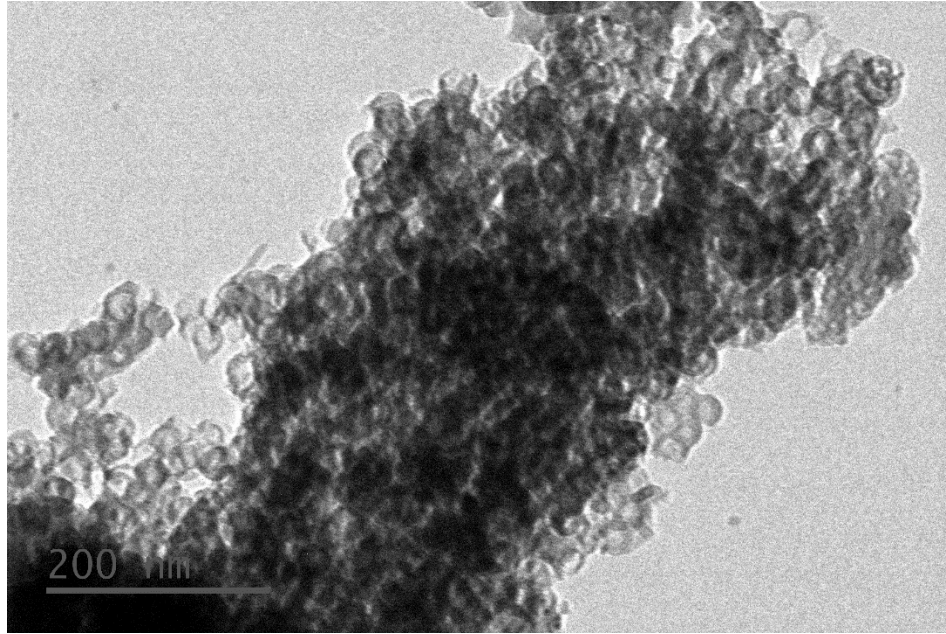


**Figure 21. Magnified TEM Detail of Primary Soot Particles**

### **4.3.2 Ash Agglomerates**

In [Figure 20](#), two separate ash agglomerates are shown as large, dark particles. Between them, soot particles are collected of a much smaller scale. [Figure 22](#) shows a typical ash agglomerate taken from the GPF test case filter after regeneration. Reviewing results taken from individual component additive oils, as well as fully formulated commercial CJ-4 oil [25], the structure and scale of the particles from the GPF test case are of the magnitude expected, giving good confidence in the applicability of results obtained from this system. Typical magnitudes of ash particle size in a higher temperature, periodic test case such as used here, summarized in [Table 9](#), produce primary ash particles in the range of 1-2 $\mu\text{m}$ . [25] Particles at the larger end of this scale, such as that shown in [Figure 23](#), are more typical of a highly aged filter. Additional literature reviewed, using Focused Ion Beam (FIB) milling on various aged DPF samples, supports an average size of approximately 2 $\mu\text{m}$  for large ash agglomerates within the filter. [26]

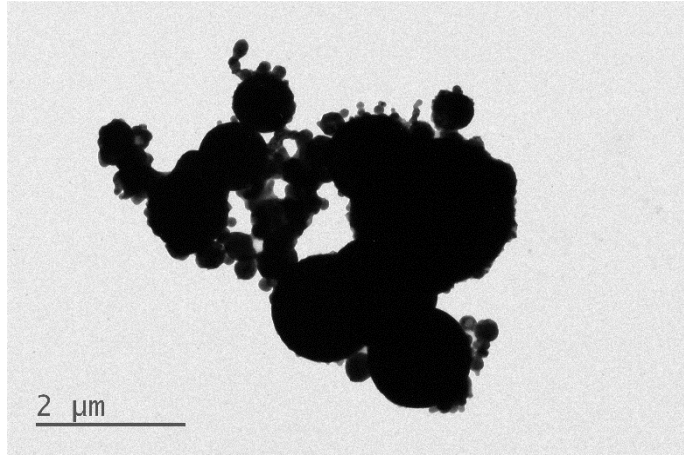


**Figure 22. Typical Ash Agglomerate from GPF Test Case**

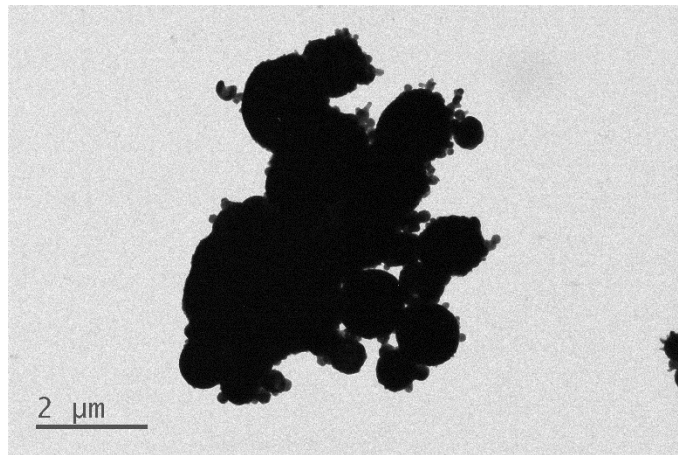


**Figure 23. Large Ash Agglomerate from GPF Test Case**

## 5 Engine Installation

In conjunction with the accelerated aging system, a Ford EcoBoost engine was installed for the purposes of developing a method to evaluate engine performance with a GPF, and in future to allow an alternate source of PM emission for aging of filters. The engine was installed alongside the accelerated aging system on a single test bed; this allowed direct connection of engine exhaust to the accelerated aging system test section, isolated by high temperature gate valves for selective use. The exhaust system is provided with a production three way catalyst, to ensure exhaust gasses at the test section are those which would be seen by a road aged filter. Both the burner and the engine share a common fuel system; the present configuration allows for independent fuel pressure regulation but not for simultaneous operation. Engine specifications are summarized in [Table 5](#); engine installation is shown in [Figure 24](#).



**Figure 24. Ford EcoBoost 1.6L Installation**

### 5.1 Support Services

The purpose of co-installing the engine is to mimic, as closely as possible, the conditions experienced in a powertrain installation on the road. Therefore, it was desired that the engine set

up be as close to a vehicle installation as possible. To facilitate this, the engine was installed using as many production components as feasible.

### **5.1.1 Fuel and Air Supply**

The installed engine is of the GDI type; as such, the engine has a camshaft driven high pressure fuel pump. Fuel is supplied to the engine in a vehicle by the lift pump; it is required to maintain a steady fuel pressure inlet to the high pressure pump of approximately 75PSI. This requirement is achieved using an external high flow automotive fuel pump, driven via a bench mounted power supply. Fuel pressure is regulated manually via a return-type fuel pressure regulator.

Engine air supply is composed of three components: cold air induction to the turbocharger, charge air supply from the turbocharger to the intake manifold via a charge cooler, and Positive Crankcase Ventilation (PCV). Cold air induction is provided from the test cell air receiver, which allows external monitoring of engine air flow; the inlet to the turbocharger is provided with a machined mounting boss to facilitate the installation of a production Manifold Absolute Pressure (MAP) sensor.

Charge air supply is provided via a custom fabricated series of aluminum pipes; the pipes are of 2.5" internal diameter and mandrel bent, seamless construction. Connections are made using smooth high pressure silicone fittings. The intake charge is cooled in a vehicle installation using an air-to-air intercooler mounted behind the front fascia, where vehicle motion generates significant airflow to cool the charge; in a laboratory setting, the use of air to cool the charge is not practical and therefore an air-to-water intercooler is provided here, cooled by building water. The intercooler is provided with a machined mounting boss to facilitate the installation of a production Temperature/Manifold Absolute Pressure (TMAP) sensor; the MAP and TMAP sensors are utilized by the Powertrain Control Module (PCM) to calculate airflow into the engine at a given time.

PCV service is provided to the engine in a vehicle installation by direct connection of the cylinder head cover to the air intake ducting after the air filter; this system functions to allow evacuation of any blow-by and entrained oil vapor from the crankcase of the engine without release to the atmosphere. Rather, the blow-by gas is recycled back to the intake and burned in

the engine. In the laboratory installation, PCV is routed to the test cell air receiver to facilitate proper function.

The test cell air receiver is provided with a gate valve which allows division of the engine air intake from the accelerated aging system; this valve prevents the engine from pulling air backwards through the burner combustion chamber during operation.

### **5.1.2 Accessory Drive and Cooling System**

The EcoBoost 1.6L engine utilized is normally fitted into a Ford Escape compact SUV; in this installation, the engine is fitted with a belt driven water pump, alternator and air conditioning compressor; these accessories take power directly from the crankshaft. In order to maintain near-vehicle conditions, the crankshaft drives the engine water pump and alternator in the test cell installation as well. The alternator provides token resistance, as no electrical load is present. An air conditioning compressor cannot be practically fitted in a test cell scenario; this accessory has been bypassed.

The vehicle cooling system normally utilizes a close-coupled radiator to cool the engine, and provides a pressurized expansion tank to purge any air from the cooling system and allow for changes in coolant volume with temperature. In the test cell, the engine is instead connected to a large pressurized coolant reservoir, with the coolant return from the engine passing through a heat exchanger which is cooled using building water. Because the reservoir is mounted remotely from the engine, a centrifugal coolant make-up pump is used to compliment the engine driven pump in overcoming the additional pumping head required. Engine coolant temperature is regulated via PCM controlled solenoid valves and the engine mechanical thermostat, identically to a vehicle installation.

### **5.1.3 Power Dissipation and Engine Starting**

The test cell is provided with a standard eddy current type magnetic air gap dynamometer rated at 200HP and 5000RPM. The dynamometer clutch is cooled using a pressurized, gravity return, closed cooling system; heat is rejected to building water via a heat exchanger. Dynamometer control is configured to dissipate power at a set RPM dictated by the user.

The dynamometer is also equipped with an AC motor, which provides for motoring capability; this motor can be used to hold an engine at a set RPM minimum; in this case, the motoring capability is provided specifically for engine starting. The engine is not provided with a starter motor due to insufficient house electrical supply to support it.

#### **5.1.4 Engine Electrical Control**

An electrical harness from a manual transmission equipped Ford Escape was used to integrate the engine and PCM into the test cell; this eliminated the need to have a Transmission Control Module (TCM). The PCM provided is of a special development type, fitted with a serial interface for use with real time data collection software described in the next section.

The engine is provided electrical power via a 30 amp bench type power supply. Using the specific wiring installation schematics for a 1.6L EcoBoost Escape, seven power inputs were identified to the engine harness to enable complete engine and PCM function. Two of these power supplies are permanent on, fused sources supplied directly from the battery in a vehicle. The third circuit is normally provided to the PCM by the Body Control Module (BCM); this circuit enables the PCM when a user keys the ignition to the “ON” position. The remaining four circuits are controlled in a vehicle by the main power relay, which closes and provides power when the user keys the ignition to the “RUN” position; this relay was retained in the test cell wiring. By separating the “ON” and “RUN” positions, the engine computer may be monitored and the engine stopped and started without loss of active data acquisition connection.

#### **5.1.5 Instrumentation**

As in most fuel injected engine installations, the vast majority of engine parameters are monitored internally via the PCM, and this information may be accessed through the serial data interface installed in the development PCM module. The only independent instrumentation installed is a thermocouple monitoring Exhaust Gas Temperature (EGT) at the inlet of the turbocharge turbine; steady state dyno operation runs the risk of potentially overheating the turbine bushings and damaging the turbocharger. For safety purposes, EGT temperatures are considered high at 1173 K (900°C), and the engine enters a self-protection mode at 1223 K (950°C); close monitoring of EGT prevents this from occurring.

## **5.2 Engine Control**

The engine is controlled via a software packaged called Vision, which is a proprietary platform developed by Accurate Technologies, Incorporated (ATI). The development PCM provided has a specific ATI interface installed, which allows direct communication via USB with the test cell computer. Due to the extended distance between the PCM and the test cell computer (26 feet, normal vehicle installations are on the order of 5 feet), a powered signal booster was also required for proper function of this system.

The PCM comes calibrated for a standard vehicle installation from the manufacturer; for dyno testing purposes, a calibration provided by Ford was flashed to the PCM via the Vision software to allow full user control of the engine. This calibration disables many engine security and safety parameters, allowing for a wide range of test protocols to be used.

Engine control is achieved by varying a series of parameters within Vision; specifically, the user has direct control over engine throttle percentage, fuel mass delivered by injector, and engine timing. Real time feedback is provided to the user showing delivered engine power, delivered fuel pressure, exhaust air-fuel ratio, actual throttle percentage and readouts of both maximum brake torque (MBT) timing and the spark timing knock threshold. The engine is run by setting a desired RPM via the dynamometer controller, then adjusting engine throttle percentage, spark timing and fuel delivery to achieve a desired load output. The load output measurement of choice is manifold pressure; typical steady state testing can run anywhere from -20 inHg<sub>gauge</sub> to approximately 15 inHg<sub>gauge</sub>.

## **5.3 Engine Performance Evaluation Test**

Part of this study was intended to develop a method by which future testing could be conducted using the engine to evaluate performance effects from a GPF at various levels of ash and soot loading. To achieve this, the engine would be operated with 100% of the exhaust stream diverted through the GPF test section at a specified loading point and the results recorded.

The test proposed would mimic the engine break-in performance evaluation; essentially, a series of tests at increasing load and RPM each held for a specific period of time. The same test would be repeated at a pre-designated series of loading points; this way, the results for each engine load

setting can be plotted across the range of load points to study the engine-filter interaction. A notional proposal for such an engine test is summarized in Table 12.

**Table 12. Notional Engine Testing Program (Single Ash Load Point; MAP measured in gauge)**

Engine Speed	Low Load MAP (5 minutes)	Intermediate Load MAP (3 minutes)	High Load MAP (1 minute)
2000 RPM	-15 inHg	-7 inHg	0 inHg
2500 RPM	-15 inHg	-7 inHg	0 inHg
3000 RPM	-7 inHg	-1 inHg	5 inHg
3500 RPM	-7 inHg	-1 inHg	5 inHg
4000 RPM	-5 inHg	0 inHg	5 inHg
4500 RPM	-5 inHg	0 inHg	5 inHg
5000 RPM	-5 inHg	0 inHg	5 inHg

## **6 Results**

Once the accelerated aging system was completed, testing began for the series of GPFs described in [Table 10](#), using the simplified loading cycle summarized in [Table 9](#). As described in [Section 3.4.3](#), testing proceeded in reverse order; that is, highest ash loaded filter first. The order was reversed so that the first filter could be compared to DPF results from prior experiments for veracity, and so that a baseline for the full loading range could be established. This change led to the modification of the original test matrix, as previously described.

The initial phase of data testing, used for this study, focuses on the pressure drop behavior of GPF filters with increasing ash load. Multiple samples were taken, to both demonstrate any variance that might be present in results, and to allow future destructive analysis of the GPF to be conducted at all test load points.

### **6.1 First Test Case – 150,000 Miles Equivalent**

Testing for the 150,000 mile equivalent filter takes approximately 5 weeks of accelerated loading and is expected to consume (based on engine oil consumption as described in [Table 5](#)) 15 quarts of oil; in laboratory testing, the amount of oil consumed was about 15.5 quarts to achieve the target ash loading. Testing was conducted using the simplified 4 hour loading cycle shown in [Table 9](#), with typically either 8 or 12 hours of loading completed in a single day; pressure drop and filter reference weights were taken between loading days.

#### **6.1.1 Deranged Case – Cordierite Substrate Melting**

When post mortem analysis commenced for the first 150,000 mile equivalent sample, it was discovered that a significant volume (approximately 20%) of the internal substrate inside that filter had been melted. This has significant effect on the behavioral performance of the filter, by co-mingling inlet and outlet channels, as well as blocking off channels in both inlet and outlet directions. [Figure 25](#) shows the damaged area of the filter, after being divided into halves for post mortem analysis.

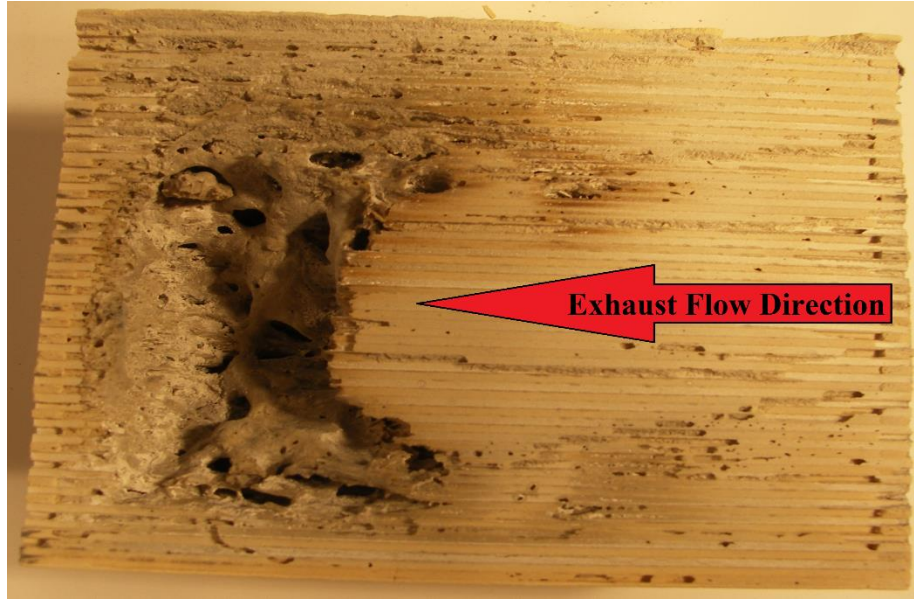


**Figure 25. Melted GPF Filter Section - 150k Miles Equivalent**

This type of damage to a filter requires a significant exothermic regeneration event to take place; cordierite has an average melting point of 1733 K (1460°C) [10], which far exceeds the normal regenerative temperature ceiling of approximately 923 K (650°C) seen during GPF operation. As discussed in [Section 2.4.2](#), this can occur if the amount of soot accumulated in the filter exceeds a threshold safety level. For GPF tests in this study, the target soot loading was 1 – 2g/L between regenerations due to increased gasoline engine sensitivity to pressure drop; this value is lower than the 5 – 6g/L typically used in DPF applications for thermal protection. [8] Because gasoline has a lower energy density than diesel fuel, it was expected that this soot load ceiling would provide adequate thermal protection for the filter substrate.

During the loading of the 150,000 mile equivalent sample, the expected soot load level was exceeded when the filter load was approximately 10g/L of ash; the pressure drop between regenerations was higher than normal on this particular loading day, which led to a decreased flow rate and increased soot production rate during that period. This led to the discovery of a GPF accelerated aging system limitation – the system has difficulty generating sufficient temperature to oxidize trapped soot within the filter when pressure drops become too high. The highly soot loaded filter was initially regenerated using a hot air flow bench, which mimics exhaust temperature and flow in an oxygen rich environment; the regeneration was completed

using the accelerated aging system. The filter exhibited a loss of computed PM load after this event, as well as an unanticipated decrease in cold flow pressure drop; these are both good indicators of internal filter damage. By dividing the filter pressure drop data over the entirety of the aging process, it is possible to pinpoint the excessive temperature event; this is shown in [Figure 26](#).

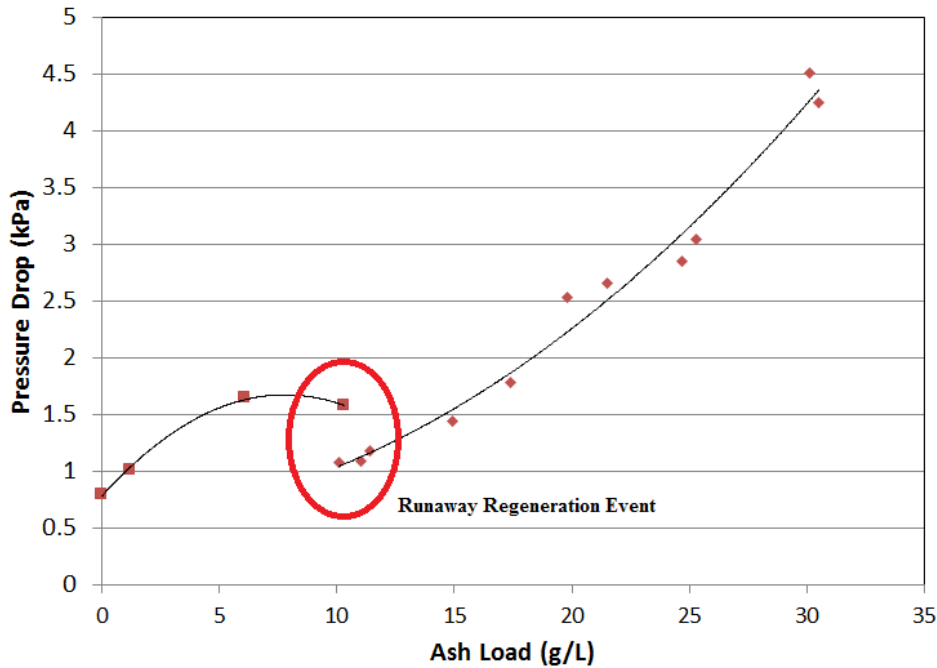


**Figure 26. 150,000 Mile Equivalent Filter Pressure Drop Summary - Melted GPF (45,000hr<sup>-1</sup>)**

The pressure drop behavior of this filter exhibits initially is consistent with the well documented transition from the deep bed filtration regime to the cake filtration regime; however, the behavior exhibited after the runaway regeneration event (approximately 10g/L ash load) is more consistent with behavior exhibited by filters with much higher ash loads [19], indicating that it is likely the filter behaved as if with a reduced volume during the later stages of loading.

### **6.1.1.1 Importance of Deranged Condition Filter Test**

While the runaway regeneration process and resulting filter damage were unintended consequences, the test is still relevant to the subject of this study: powertrain performance. Ford Motor Company has conducted a limited series of on-vehicle GPF tests in similar underbody configurations; during these tests they experienced multiple cases of filters either cracked or

damaged by a runaway regeneration process. Since filter damage is well within the realm of possibility for vehicle mounted GPFs, the decision was made to retain this filter for post mortem analysis.

### 6.1.1.2 Melted Filter Preliminary Post Mortem

In order to help characterize the behavior of a filter subject to melting or other thermal damage, closer examination of ash particles and filter – ash interactions was desirable. Using a combination of FIB and Scanning Electron Microscopy (SEM) imaging techniques, detailed examination was made of both melted and intact regions of the 150,000 mile equivalent filter. Immediately evident in the melted region is that significant cracking is evident in the filter substrate; additionally, it is apparent that local surface porosity of the filter increases during the melt event. [Figure 27](#) shows these effects; surface porosity may be compared to that seen in a clean GPF as shown in [Figure 3](#).

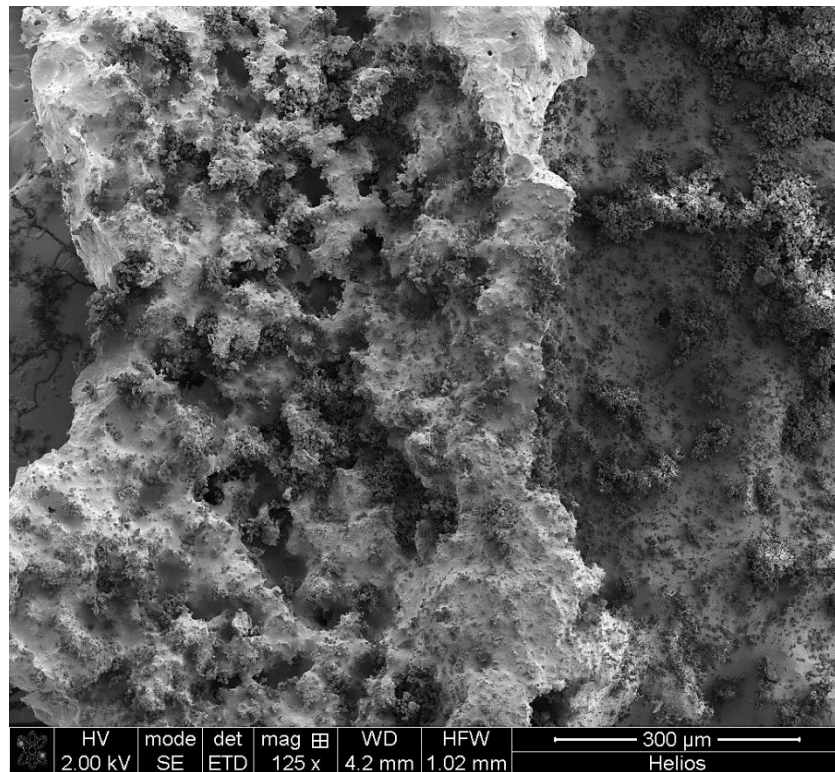


**Figure 27. GPF Surface in Melted Region Showing Cracking (left) and Increased Porosity (center)**

Upon closer examination of the melted filter surface, it may also be observed that the surface roughness in the melt region is evidently less than that of the clean GPF; it is also apparent that primary ash particles have undergone some level of sintering in the melt region. [Figure 28](#) shows the localized roughness reduction around a single pore on the GPF, with a collection of sintered ash particles.

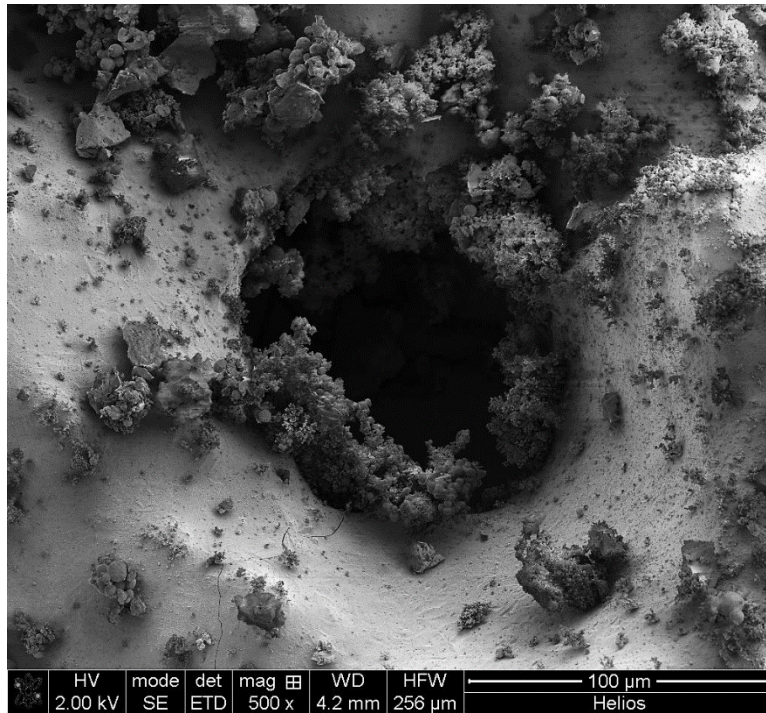


**Figure 28. Individual Pore of GPF Surface in Melt Region**

Additionally, it is apparent in [Figure 28](#) that there may be some level of chemical interaction between the surface of the GPF and the ash particles inside the melt region; this suggests a potential chemical binding phenomena in this region which is not observed in the intact region. Closer analysis of the particles inside this region shows a large amount of surface roughness on the sintered primary ash particles; this effect is shown in [Figure 29](#).

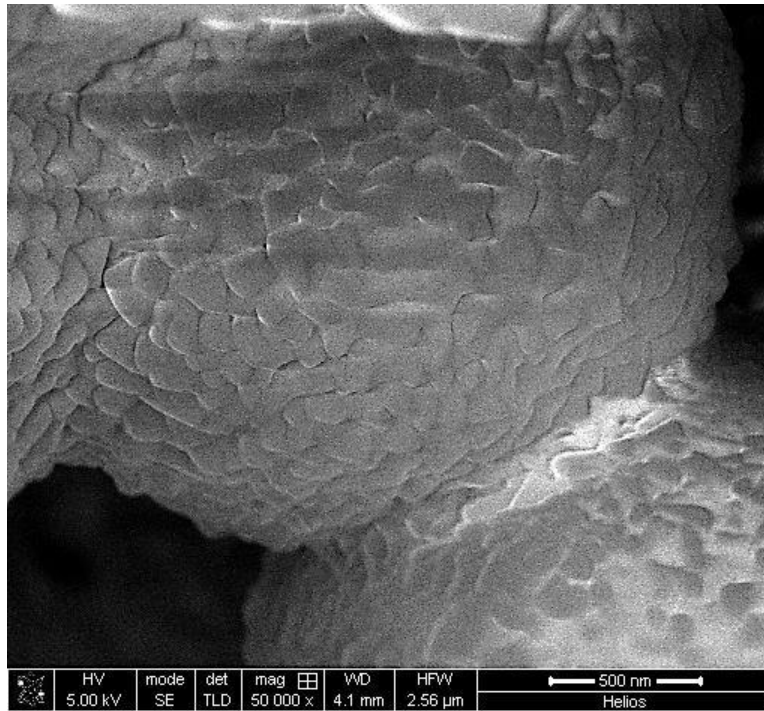


**Figure 29. Sintered Primary Ash Particles in Melt Region**

Using FIB milling, two interesting phenomena may be observed in the primary ash particles in the melt region. The first is that the larger ash agglomerates have a tendency to become shells, rather than solid masses; this suggests some effect on the formation of ash particles during the melt event. Secondly, the smaller primary ash particles exhibit a complex interior structure, rather than being solid; again, this suggests some level of chemical alteration to the ash in this region. Both of these observations are shown in [Figure 30](#).

Comparison to the intact region of the GPF are informative to better understand the effects illustrated; [Figure 31](#) shows an individual filter pore in the intact region of the filter, both as found and after FIB milling to show ash particle structure and GPF-ash interaction. Here it may be noted that the ash appears to be exclusively above the GPF surface, with the primary mode of adhesion being the roughness of the substrate, which is evidently much greater than that shown in [Figure 28](#). Likewise, comparison between [Figure 30](#) and [Figure 31](#) allows observation of the differences in ash particle structure in the two regions of the same filter.

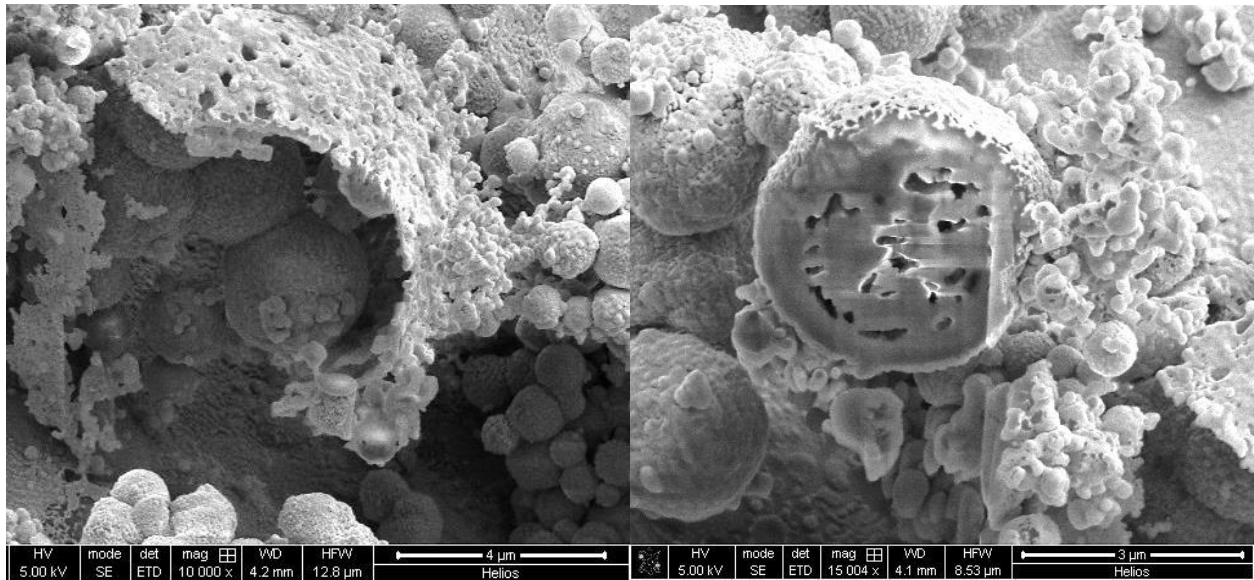


**Figure 30. Large Ash Agglomerate Showing Shell-like Structure (left) and Primary Ash Particle Cut via FIB Milling to Show Complex Internal Structure (Right); Melted Filter Region**

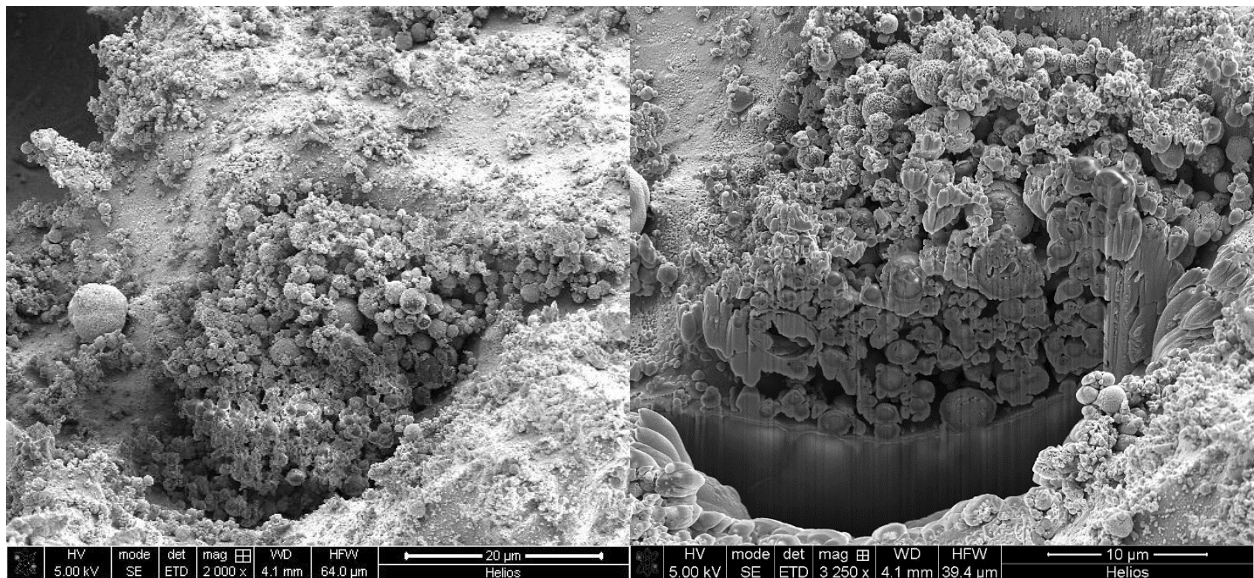


**Figure 31. Individual Filter Pore with Ash Agglomerates (Left), GPF - Ash Interaction within the Pore Shown via FIB Milling (Right); Intact Filter Region**

### 6.1.2 Undamaged 150,000 Mile Equivalent Filter

After post mortem results were taken from the initial 150,000 mile filter and the melted region discovered, a second 150,000 miles filter was loaded. This filter provides a solid basis for comparison with the deranged filter results, and also serves as the baseline to which the lower loaded filters, described in [Table 10](#), are compared. This filter exhibited pressure drop behavior

in good keeping with that expected from previous results published for DPF testing [8,11,13,18-21]; deep bed filtration is evident in early loading stages and pressure drop stabilizes in the cake filtration regime as expected. The results obtained from this filter are shown, in comparison to the deranged case, in [Figure 32](#).

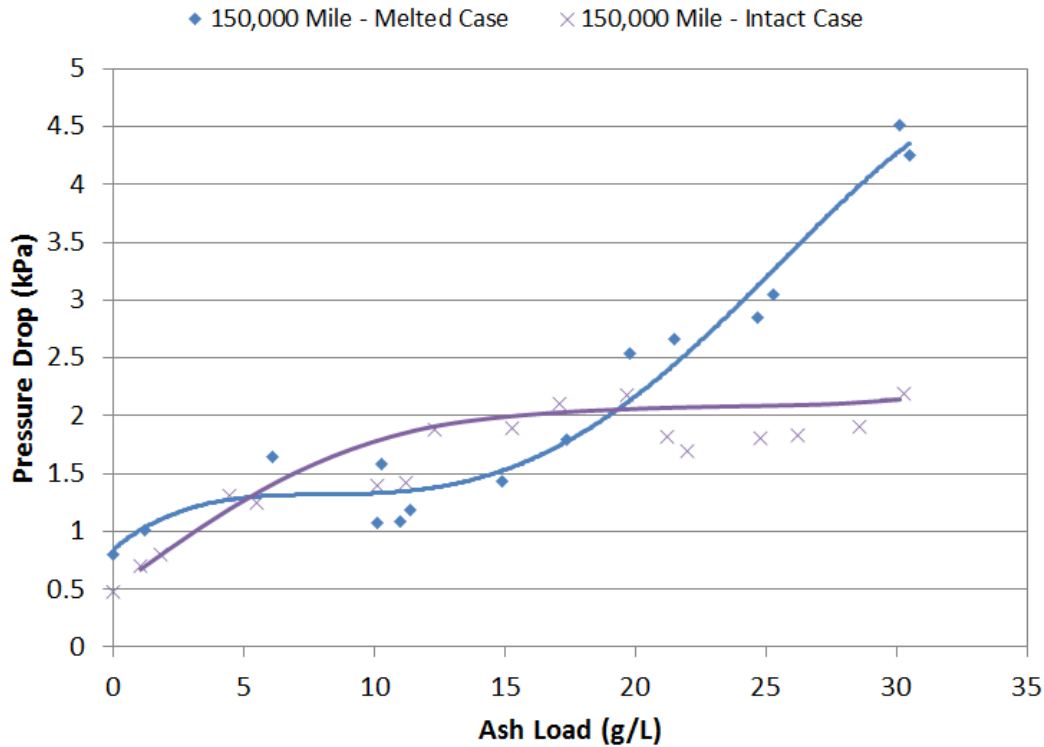


**Figure 32. Pressure Drop Comparison: 150,000 Mile Equivalent Intact vs. Melted Cases (45,000hr<sup>-1</sup>)**

## 6.2 Pressure Drop Summary of Intact Filters

Once the first test case was complete, additional samples were loaded according to the test matrix described in [Table 10](#). Due to additional time required to complete the first case (150,000 equivalent miles) because of filter damage, the order in which the filters were loaded was again modified. The second case completed was the 100,000 mile equivalent, followed by the 15,000 and 30,000 mile equivalent filters. Time to complete the test matrix ran short due to the deranged 150,000 mile test case; at the time of first phase project completion, the 60,000 mile equivalent filter sample was not completely loaded. A summary of the pressure drops for the remaining filters is provided in [Figure 33](#). The 150,000 mile deranged case, discussed in [Section 6.1.1](#), is omitted.

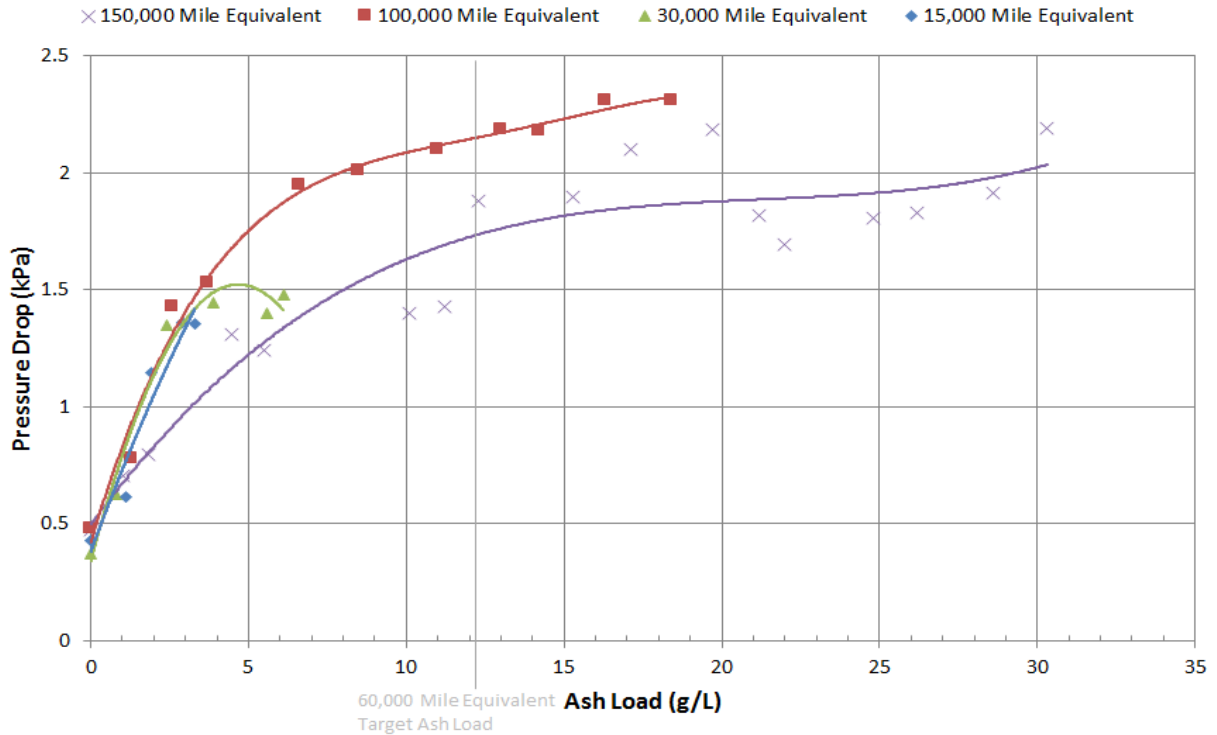


**Figure 33. Pressure Drop Summary for GPF Test Samples (45,000hr<sup>-1</sup>)**

One result which is immediately obvious is that there is some variability in the pressure drop recordings for each individual filter; the variation is more readily apparent in an amplified view of the deep bed filtration regime, shown in [Figure 34](#).

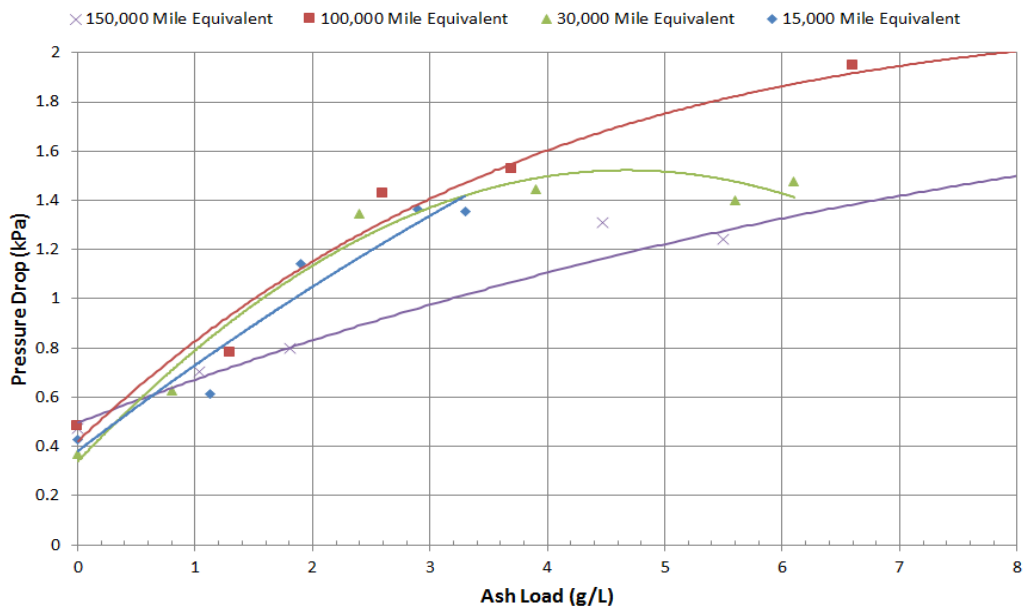


**Figure 34. Pressure Drop Summary, Deep Bed Filtration Regime (45,000hr<sup>-1</sup>)**

The variation occurs almost exclusively within the deep bed filtration regime, approximately the first 5g/L of the filter loading. Without complete post mortem analysis data, it is impossible to accurately determine the cause of these variations; however, based on recorded loading rates for each filter it is possible to hypothesize that the initial rate of loading, in g/L per hour of PM accumulated, effects the density if the initial ash layers deposited within the filter pores. Initial loading rates for the 15,000, 30,000, and 100,000 mile filters are nearly identical, approximately 0.21g/L per hour, where the 150,000 mile sample was initially aged at approximately 0.13g/L per hour.

In each case, pressure drop measurements were recorded across the full span of the system's space velocity capacity at each individual load point during the aging process. These plots give a good visual representation of the load rate on any given day for the filter; these plots are provided for each sample in the Appendix, Figures A.4 – A.7.

## **6.3 Future Work**

As previously discussed, the deranged 150,000 mile test case caused a significant shift in the project timing, due to the additional six weeks needed to create a second fully aged sample. As such, some portions of the project were shifted and were not completed within the original time spectrum allotted. These components will be the first completed in the future; specifically, to complete the original test sequence, the 60,000 mile equivalent filter must be fully aged.

### **6.3.1 Post Mortem Analysis**

Once all five test filters are completed, there is much further information to be gained through post mortem analysis. Some of the techniques used here for system validation, including TEM, SEM, and FIB Milling, are valuable tools for additional data collection from the filter samples. Additionally, X-Ray Diffraction (XRD) will be used to determine elemental composition of the ash contained within the filters, and to assess transport of individual lubricating oil components within the GPF.

One of the specific future goals that developed from this project is the further utilization of the 3DCT scanning technology which has become available; specifically, this tool stands to provide much better detail and accuracy in determining ash packing density, ash layer thickness, ash plug

length, and ash porosity. The current method used to determine these quantities is strictly mechanical; each filter is divided into core sections using a ceramic cutting tool, and then digital photographs are taken of the wall of the exposed channels. From digital image measurement tools, it is possible to determine layer thickness and ash plug length as well as porosity; once this is complete, the ash can be mechanically scraped from the GPF sample and weighed, allowing calculation of ash density. These methods have proven to give reasonable results, but are time consuming and highly susceptible to error if not performed flawlessly. Future work intends to take high resolution 3DCT imagery of an aged GPF sample, use of image measurement correlation to calculate parameters, and then calculation the relevant quantities using the mechanical methods, to compare results and allow refinement of the 3DCT calculation process.

### **6.3.2 Laboratory vs. Engine Particulate Matter Comparison**

Results obtained from the accelerated aging system compared well with those from other laboratory systems and with road aged DPF filter results; however, there is little knowledge or data available on analysis of PM captured in GPFs. Therefore, one of the future phases of this project would contain an in-depth analysis on an elemental level of the ash and soot particles obtained from the EcoBoost engine and the accelerated aging system. Comparison of elemental composition, density, average size scales and particulate structure are all important to understanding the fundamental behavior of GPFs; the information gathered in this analysis will provide much needed data for future GPF design and evaluation.

### **6.3.3 Powertrain Performance Analysis**

Part of a robust design program is the ability to thoroughly test proposed design changes prior to implementation; one of the future goals derived from this study is the ability to offer engine performance effects analysis of a GPF sample simultaneously with accelerated aging. The notional engine testing matrix proposed in [Table 12](#) will be used to initiate this evaluation; once sufficient data is collected from this type of testing, the potential exists to develop a mathematical model to simulate GPF behavioral effects on a powertrain. Additionally, this capability will allow for controlled soot loading of a filter, both to determine a safe thermal loading limit to prevent filter melting, and to better understand the requirements for regeneration which will be present in a GDI powertrain installation.

(This Page Intentionally Left Blank)

## **7 Conclusions**

The major stated goal of this project phase was to create and validate an operational system for the accelerated aging of particulate filters using gasoline as a fuel. Through significant modification to an existing M.I.T. design for DPF aging, the system was constructed and installed in the automotive lab with a collocated GDI engine provided by Ford Motor Company.

### **7.1 Confirmation of Particulate Emission Characteristics**

Preliminary analysis of soot and ash particulate samples collected from the accelerated aging system correlate well with the expected structure and size of the particles found in previous studies. [25,26]

### **7.2 Validation of Equivalent Mileage Calculations**

The approximate equivalent mileage calculation discussed in [Section 2.2.2](#) and provided as [Equation 6](#) proved to provide a good first principles data point on which to base filter loading points; laboratory oil consumption to obtain the desired ash loading, as discussed in [Section 6.1](#), was within 3% of the stated engine oil consumption for the same mileage.

### **7.3 Substantiation of GPF similarity to DPF**

GPF pressure drop behavior, as examined over four different test filters in this study, proved to be substantially similar to DPF behavior under similar loading circumstances. This is a critical result, as it gives credence to the supposition that GPF behavior ought to be substantially the same as DPF [9], and therefore the large body of published knowledge on DPF behavior can be tapped as a source for future experimental work with GPFs.

### **7.4 Validation of Accelerated Aging System as Viable Test Platform**

The accelerated aging system proved to provide reliable, safe aging of GPF samples using gasoline as a fuel and conventional motor oil for ash loading; this system remains fully operational and is being utilized for future GPF studies. The system provides capability to load GPFs through a range of airflows, temperatures and soot loading levels necessary to fully document the behavior of the filters under varied conditions.

## **7.5 Project Continuation**

While the complete test matrix originally outlined in Table 10 was not completed during the course of this study as discussed in Section 6.2, the results obtained show much promise in the accelerated aging system. Completion of the original test matrix and continuation of post mortem filter analysis will provide additional beneficial conclusions for the ongoing study of GPF behavior, and future work which derives from the difficulties encountered and conclusions drawn here provide basis for a robust research program going forward.

Near term increases in the stringency of emissions regulations, particularly applicable to GDI engines both in the United States and Europe, are ample motivation for practical application of the findings of this study and future work as well. With continued process development and further system validation, the accelerated aging system constructed here and co-located with the GDI engine stands to provide a robust, rapid testing platform for applicable real-world solutions to meeting proposed and future emissions regulations.

## REFERENCES

- 
- <sup>1</sup> Piock, W., Hoffmann, G., Berndorfer, A., Salemi, P. et al., "Strategies Towards Meeting Future Particulate Matter Emission Requirements in Homogeneous Gasoline Direct Injection Engines," *SAE Int. J. Engines* 4(1):1455-1468, 2011, doi:10.4271/2011-01-1212.
- <sup>2</sup> Heywood, J. B., Internal Combustion Engine Fundamentals, McGraw-Hill, Inc., New York, 1988.
- <sup>3</sup> Fraser, N., Blaxill, H., Lumsden, G., and Bassett, M., "Challenges for Increased Efficiency through Gasoline Engine Downsizing," *SAE Int. J. Engines* 2(1):991-1008, 2009, doi:10.4271/2009-01-1053.
- <sup>4</sup> Velji, A., Yeom, K., Wagner, U., Spicher, U. et al., "Investigations of the Formation and Oxidation of Soot Inside a Direct Injection Spark Ignition Engine Using Advanced Laser-Techniques," SAE Technical Paper 2010-01-0352, 2010, doi:10.4271/2010-01-0352.
- <sup>5</sup> United States Environmental Protection Agency, "Control of Air Pollution from Motor Vehicles: Tier 3 Motor Vehicle Emission and Fuel Standards," 40 CFR Parts 79, 80, 85, 86, 600, 1036, 1037, 1039, 1042, 1048, 1054, 1065, and 1066 [Docket EPA-HQ-OAR-2011-0135; FRL 9906-86-OAR] RIN 2060-AQ86 [Online]. Available: <http://www.epa.gov/otaq/documents/tier3/tier-3-fr-preamble-regs-3-3-14.pdf> [Accessed: 26MAR2014]
- <sup>6</sup> European Commission, "Commission Regulation (EU) No 459/2012 of 29 May 2012 amending Regulation (EC) No 715/2007 of the European Parliament and of the Council and Commission Regulation (EC) No 692/2008 as regards emissions from light passenger and commercial vehicles (Euro 6) Text with EEA relevance," OJ L 142, 01/06/2012, p. 16–24. Available: [http://eur-lex.europa.eu/legal-content/EN/ALL/?uri=uriserv:OJ.L\\_.2012.142.01.0016.01.ENG](http://eur-lex.europa.eu/legal-content/EN/ALL/?uri=uriserv:OJ.L_.2012.142.01.0016.01.ENG) [Accessed: 16APR2014]
- <sup>7</sup> Kirchner, U., Vogt, R., and Maricq, M., "Investigation of EURO-5/6 Level Particle Number Emissions of European Diesel Light Duty Vehicles," SAE Technical Paper 2010-01-0789, 2010, doi:10.4271/2010-01-0789.
- <sup>8</sup> Sappok, A. and Wong, V., "Ash Effects on Diesel Particulate Filter Pressure Drop Sensitivity to Soot and Implications for Regeneration Frequency and DPF Control," *SAE Int. J. Fuels Lubr.* 3(1):380-396, 2010, doi:10.4271/2010-01-0811
- <sup>9</sup> Steimle, F., Kulzer, A., Richter, H., Schwarzenhal, D. et al., "Systematic Analysis and Particle Emission Reduction of Homogeneous Direct Injection SI Engines," SAE Technical Paper 2013-01-0248, 2013, doi:10.4271/2013-01-0248.
- <sup>10</sup> Ricoult, D., "Materials Engineering and New Designs for Robust Cordierite Diesel Particulate Filters," SAE Technical Paper 2005-26-024, 2005, doi:10.4271/2005-26-024.
- <sup>11</sup> Konstandopoulos, A., Zarvalis, D., Kladopoulou, E., and Dolios, I., "A Multi-Reactor Assembly for Screening of Diesel Particulate Filters," SAE Technical Paper 2006-01-0874
- <sup>12</sup> Konstandopoulos, A., Kostoglou, M., Skaperdas, E., Papaioannou, E. et al., "Fundamental Studies of Diesel Particulate Filters: Transient Loading, Regeneration and Aging," SAE Technical Paper 2000-01-1016, 2000, doi:10.4271/2000-01-1016.

- 
- <sup>13</sup> Bodek, K. and Wong, V., "The Effects of Sulfated Ash, Phosphorus and Sulfur on Diesel Aftertreatment Systems - A Review," SAE Technical Paper 2007-01-1922
- <sup>14</sup> Delvigne, T., "Oil Consumption Sources in a Modern Gasoline Engine Including Contribution of Blow-by Separator and Turbocharger: An Experimental Study Based on the Use of Radiotracers," *SAE Int. J. Fuels Lubr.* 3(2):916-924, 2010, doi:10.4271/2010-01-2256
- <sup>15</sup> Yilmaz, E., Tian, T., Wong, V., and Heywood, J., "The Contribution of Different Oil Consumption Sources to Total Oil Consumption in a Spark Ignition Engine," SAE Technical Paper 2004-01-2909, 2004, doi:10.4271/2004-01-2909.
- <sup>16</sup> Manni, M., Pedicillo, A., and Bazzano, F., "A Study of Lubricating Oil Impact on Diesel Particulate Filters by Means of Accelerated Engine Tests," SAE Technical Paper 2006-01-3416
- <sup>17</sup> Watson, S., Huang, W., and Wong, V., "Correlations among Ash-Related Oil Species in the Power Cylinder, Crankcase and the Exhaust Stream of a Heavy-Duty Diesel Engine," SAE Technical Paper 2007-01-1965, 2007, doi:10.4271/2007-01-1965.
- <sup>18</sup> Sappok, A., Santiago, M., Vianna, T., and Wong, V., "Characteristics and Effects of Ash Accumulation on Diesel Particulate Filter Performance: Rapidly Aged and Field Aged Results," SAE Technical Paper 2009-01-1086, 2009, doi:10.4271/2009-01-1086.
- <sup>19</sup> Sappok, A., Rodriguez, R., and Wong, V., "Characteristics and Effects of Lubricant Additive Chemistry on Ash Properties Impacting Diesel Particulate Filter Service Life," *SAE Int. J. Fuels Lubr.* 3(1):705-722, 2010, doi:10.4271/2010-01-1213
- <sup>20</sup> Sappok, A. and Wong, V., "Detailed Chemical and Physical Characterization of Ash Species in Diesel Exhaust Entering Aftertreatment Systems," SAE Technical Paper 2007-01-0318, 2007, doi:10.4271/2007-01-0318.
- <sup>21</sup> Sappok, A., Beauboeuf, D., and Wong, V., "A Novel Accelerated Aging System to Study Lubricant Additive Effects on Diesel Aftertreatment System Degradation," *SAE Int. J. Fuels Lubr.* 1(1):813-827, 2009, doi:10.4271/2008-01-1549
- <sup>22</sup> Hepburn, J., Dobson, D., Hubbard, C., and Otto, K., "The Pulse Flame Combustor Revisited," SAE Technical Paper 962118, 1996, doi:10.4271/962118.
- <sup>23</sup> U.S. Patent 7,625,201 B2; Ingalls, Jr. Et Al *Method and Apparatus for Testing Catalytic Converter Durability* [Online]. Available: <http://patft.uspto.gov/netacgi/nph-Parser?Sect1=PTO2&Sect2=HITOFF&p=1&u=%2Fnetacgi%2FPTO%2Fsearch-bool.html&r=2&f=G&l=50&co1=AND&d=PTXT&s1=%227,625,201+B2%22&OS=%227,625,201+B2%22&RS=%227,625,201+B2%22> [Accessed: 09APR2014]
- <sup>24</sup> Bardasz, E., Cowling, S., Panesar, A., Durham, J. et al., "Effects of Lubricant Derived Chemistries on Performance of the Catalyzed Diesel Particulate Filters," SAE Technical Paper 2005-01-2168, 2005, doi:10.4271/2005-01-2168.

---

<sup>25</sup> Kamp, C., Sappok, A., Wang, Y., Bryk, W. et al., "Direct Measurements of Soot/Ash Affinity in the Diesel Particulate Filter by Atomic Force Microscopy and Implications for Ash Accumulation and DPF Degradation," *SAE Int. J. Fuels Lubr.* 7(1):307-316, 2014, doi:10.4271/2014-01-1486

<sup>26</sup> Kamp, C., Sappok, A., and Wong, V., "Soot and Ash Deposition Characteristics at the Catalyst-Substrate Interface and Intra-Layer Interactions in Aged Diesel Particulate Filters Illustrated using Focused Ion Beam (FIB) Milling," *SAE Int. J. Fuels Lubr.* 5(2):696-710, 2012, doi:10.4271/2012-01-0836.

(This Page Intentionally Left Blank)

## APPENDIX



**Figure A. 1 Accelerated Aging System Installation**

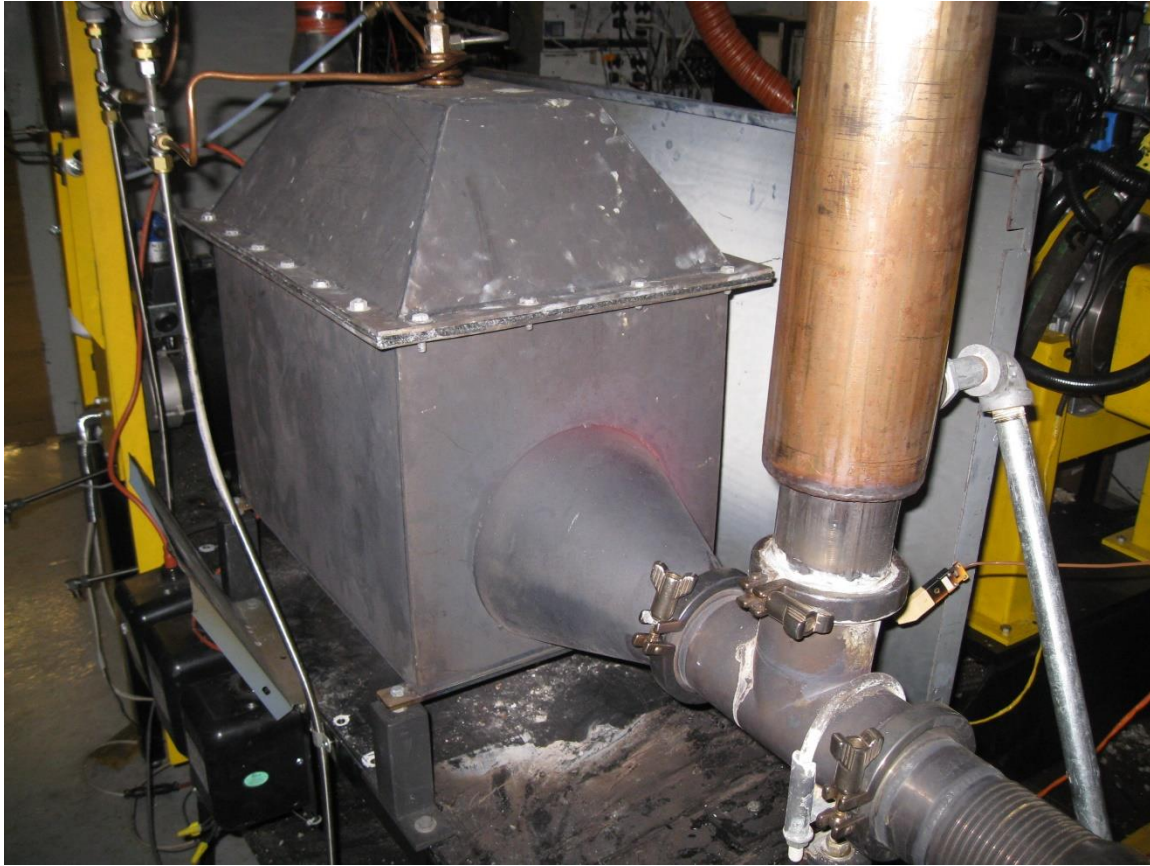


Figure A. 2 Close Up of Accelerated Aging System Combustion Chamber

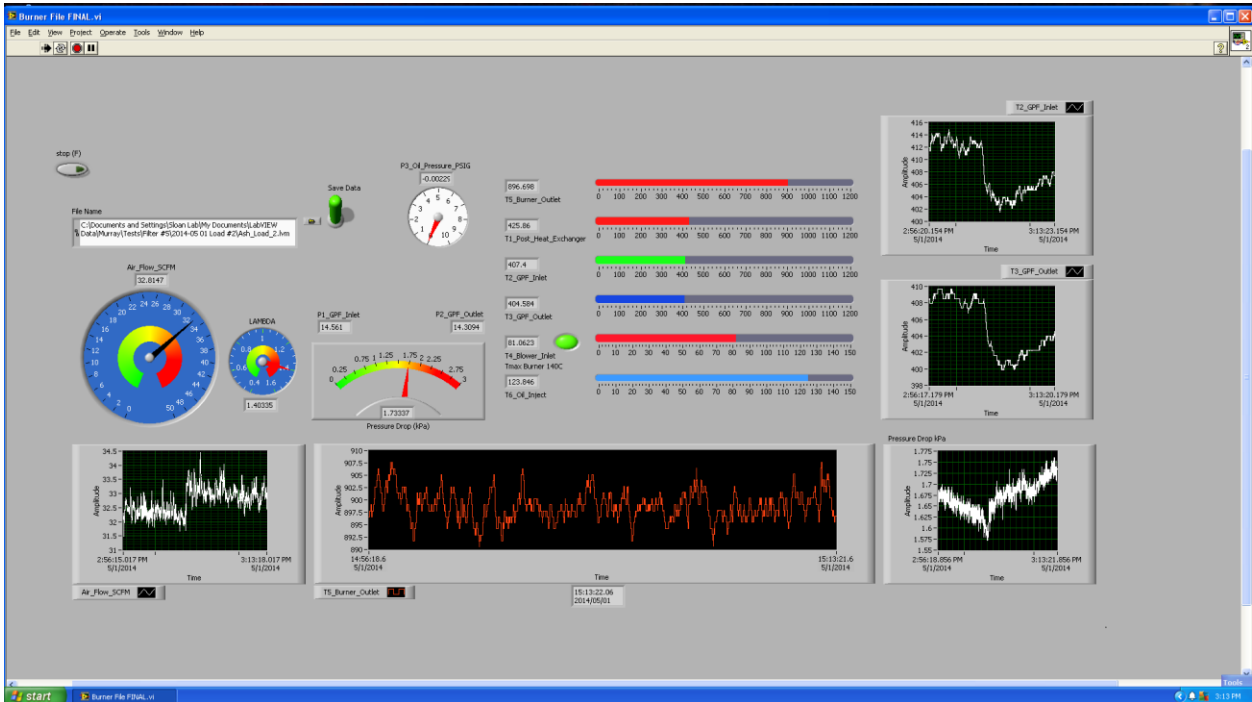


Figure A. 3 LabView Front Page Data Collection Display

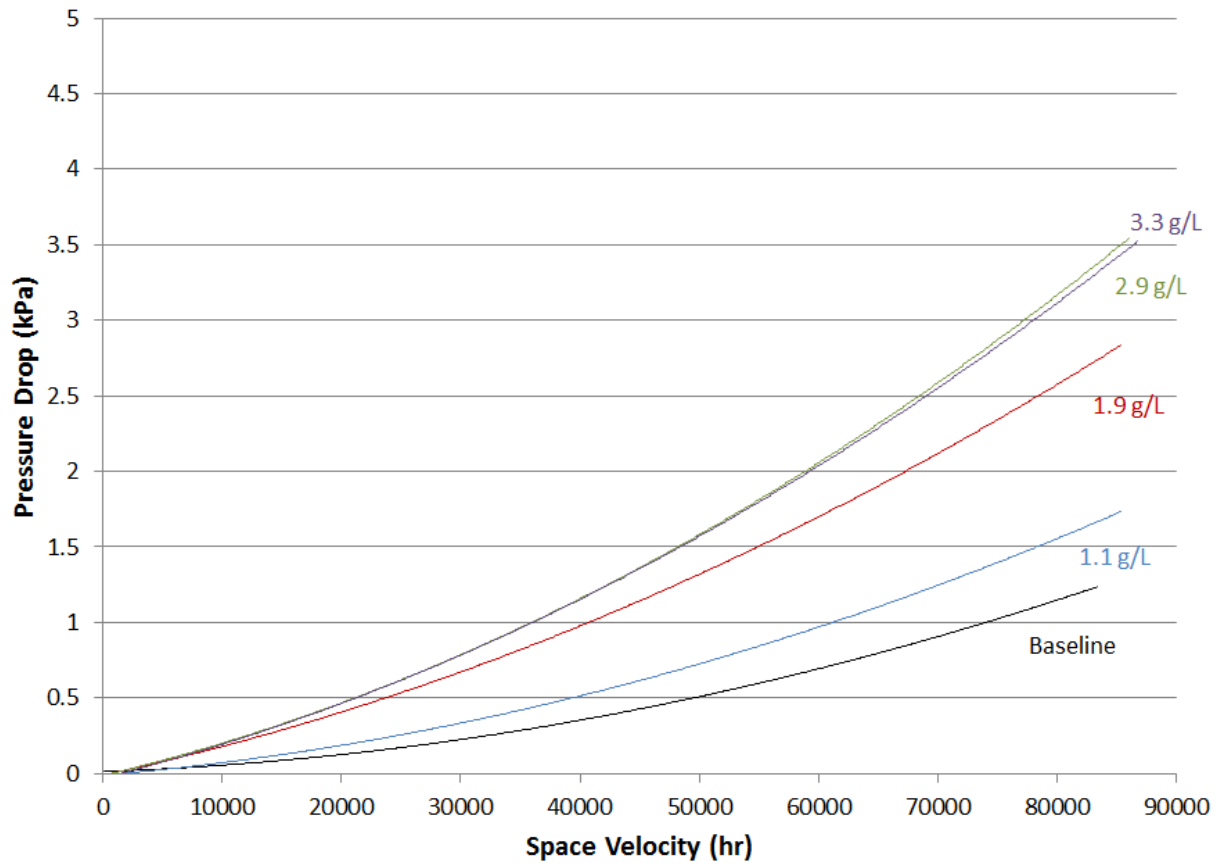


Figure A. 4 15,000 Mile Equivalent Sample Pressure Drop

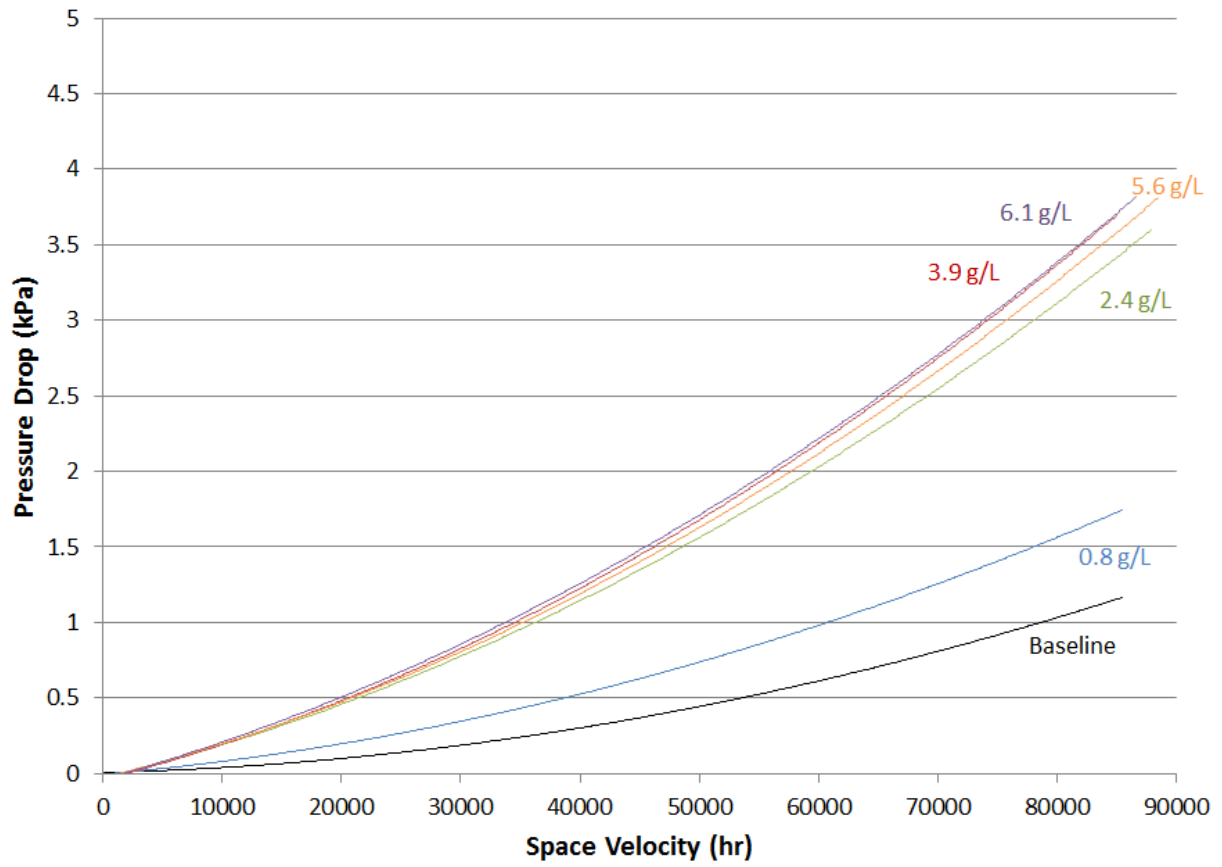


Figure A. 5 30,000 Mile Equivalent Sample Pressure Drop

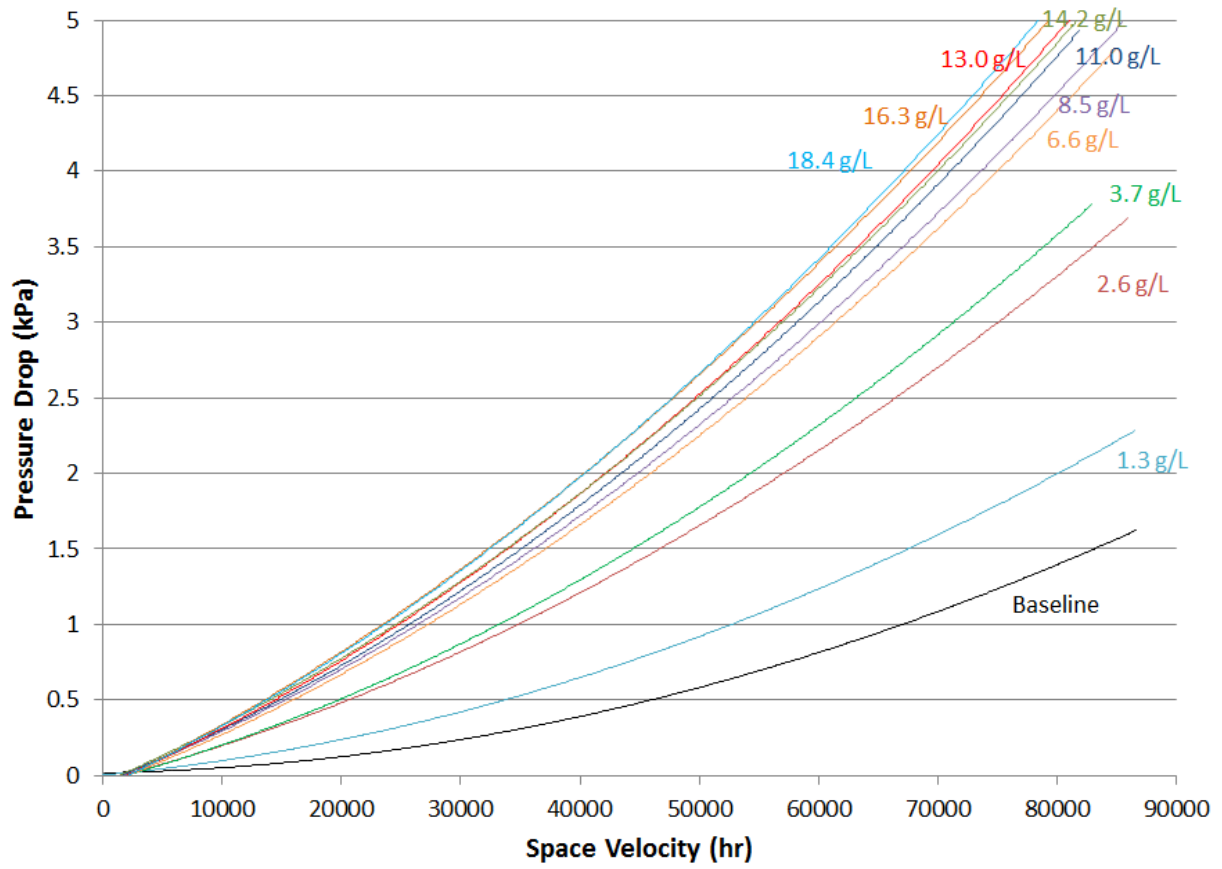


Figure A. 6 100,000 Mile Equivalent Sample Pressure Drop

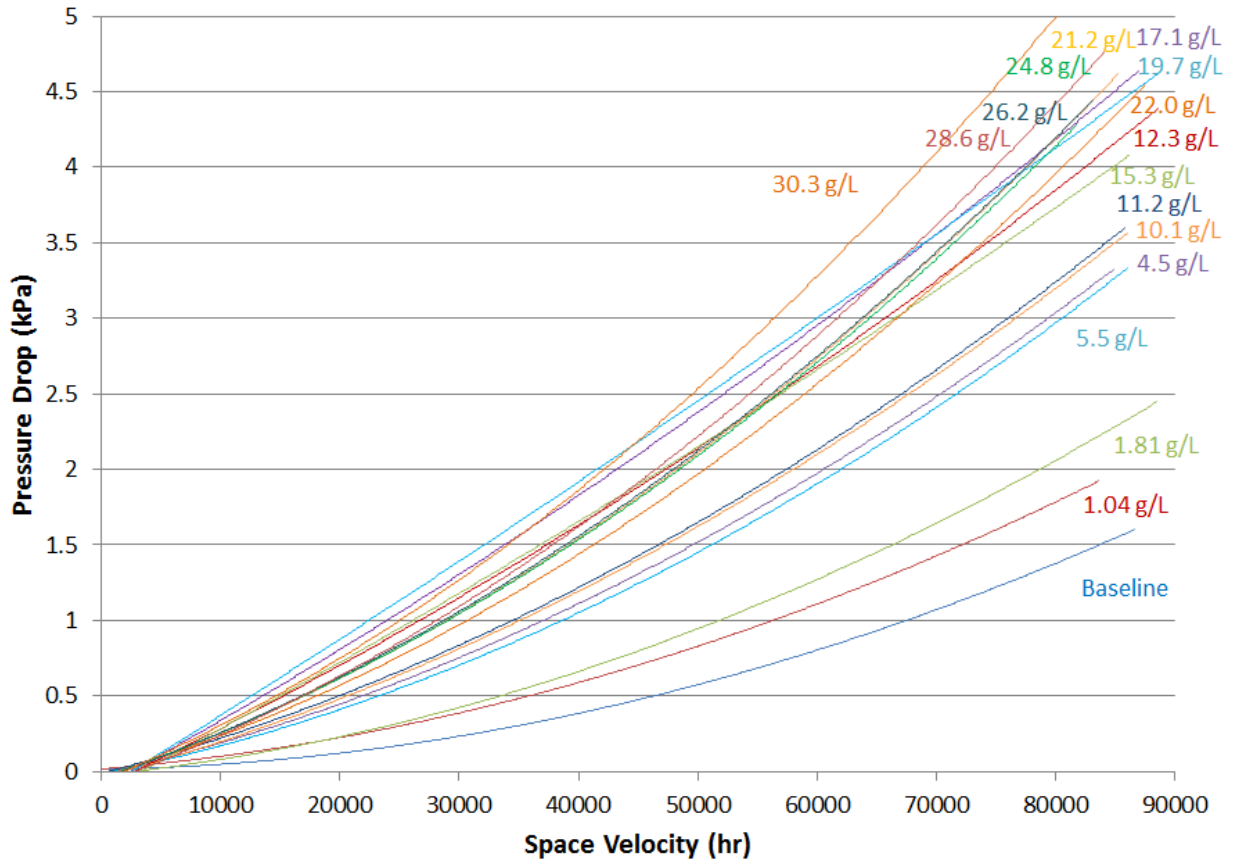


Figure A. 7 150,000 Mile Equivalent Sample Pressure Drop